AD-A035 787 PARIS-6 UNIV (FRANCE) LABORATOIRE D'OPTIQUE DES SOLIDES F/G 20/12
INVESTIGATIONS OF SURFACES AND INTERFACES USING OPTICAL EXCITAT--ETC(U)
DEC 76 F ABELES, T LOPEZ-RIOS DA-ERO-75-G-027

UNCLASSIFIED NL

1 OF 1
ADA035787

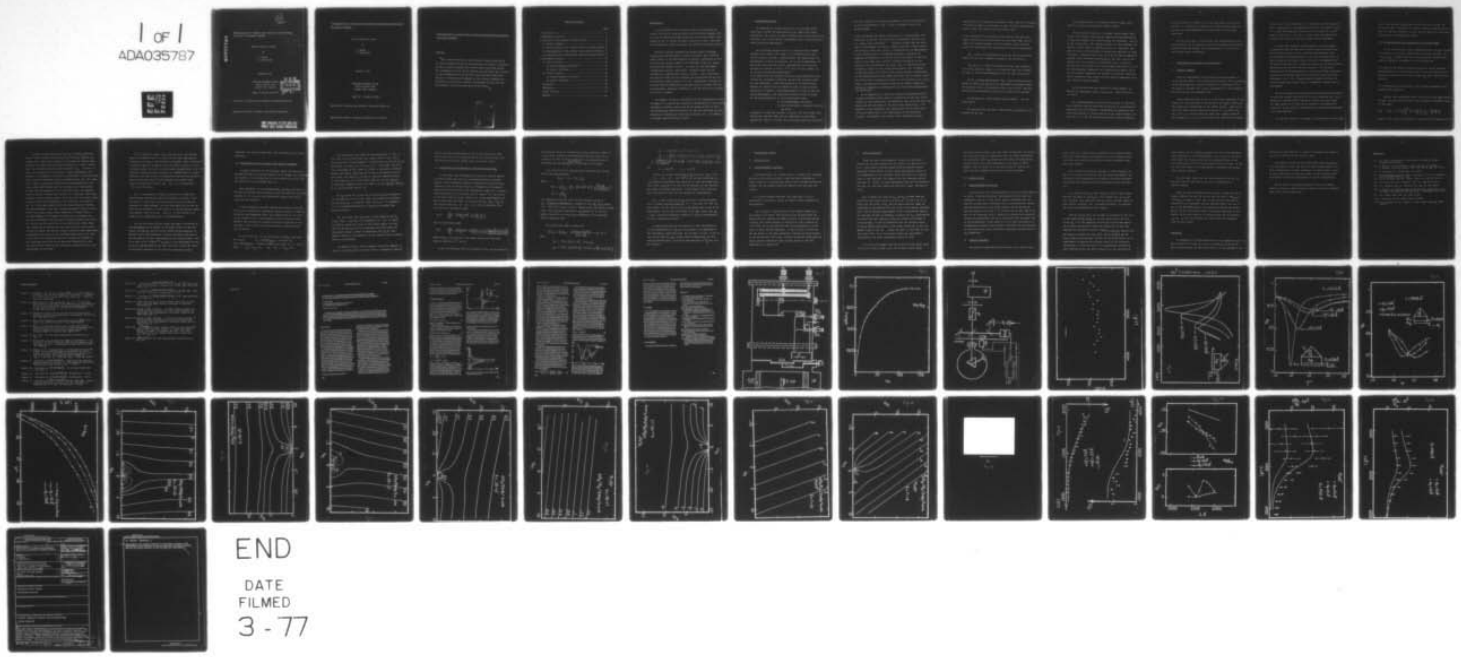

END

DATE
FILMED
3-77

(12) NW

INVESTIGATIONS OF SURFACES AND INTERFACES USING OPTICAL EXCITATION OF SURFACE PLASMONS

Annual Technical Report

by

F. ABELES
T. LOPEZ-RIOS

December 1976

EUROPEAN RESEARCH OFFICE
United States Army
London, NW1, England

GRANT N° DA-ERO-75-G-027

Laboratoire d'Optique des Solides, Université Paris VI

Investigations of Surfaces and Interfaces Using Optical Excitation of Surface Plasmons

Annual Technical Report

by

F. ABELES
T. LOPEZ-RIOS

December 1976

EUROPEAN RESEARCH OFFICE
United States Army
London, NW1, England

GRANT N° DA-ERO-75-G-027

Laboratoire d'Optique des Solides, Université Paris VI

Investigations of Surfaces and Interfaces Using Optical Excitation of Surface Plasmons

Abstract

This report presents the application of optical excitation of surface plasmons by ATR to investigations of metallic adsorption on metal surfaces prepared and studied under ultra-high vacuum. The experimental set-up and the methods are described. The accuracy of the determination of the surface layer effective dielectric constant is duscussed and compared to the accuracy obtained by a differential reflection technique. Preliminary results for very thin deposits of Au on Ag and Ag on Au are given.

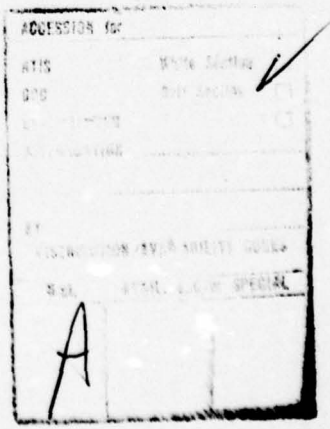

Table of Contents

Introduction

In the DA-ERO-75-G-02 technical report, we presented the results obtained by using optically excited surface plasmons (SP) to study the gold-electrolyte interface in the ionic double layer region as well as during the anodic oxydation of gold. This work was performed for fixed wavelength and variable electrode potential

Metallic surfaces prepared and studied under ultra-high vacuum conditions represent a simpler situation. This technical report refers to the investigation of metallic adsorption of gold on silver and silver on gold in the 4000-6000 Å spectral region. For practical reasons, we use , to excite SP, the Kretschmann configuration (prism - metal film - vacuum) rather than the original Otto configuration (prism - vacuum - metal substrate). The metallic films which we consider are polycrystalline but the microcrystals always present a (1,1,1) preferential orientation and have lateral dimensions of the same order or greater than the film thickness. Generally speaking, we can say that we are looking at a (1,1,1) surface.

In chapter 1 we give a description of the experimental set-up. In chapter 2 we discuss the accuracy of determination of the optical constants of surface layers with the SP method as well as with the differential reflection method. We consider different possible situations: absorbing on reflecting substrate, ect... In chapter 3, we present some preliminary results.

1 Experimental set-up

The experimental set-up consists of an ultra-high vacuum system which allows the preparation of the samples by vacuum evaporation, the control of their thickness and of their electrical resistance and in situ optical measurements with a specially built double-beam spectrophotometer.

The ultra-high vacuum system is a stainless-steel chamber equipped with a 200 l ionic pump, a Ti sublimation pump and a liquid nitrogen cryotrap. A Bayard-Alpert type gauge allows the measurements of the total pressure. In our first experiments, we have used viton rings for faster experimental cycles and the pressure was limited to about 5.10^{-9} torr. In this chamber, we can perform the following experiments:

a- We deposit the thin metallic films by vacuum evaporation onto a prism and a reference substrate. We have two crucibles under the same shielding. A Sloan microbalance is situated mid way between the crucible and the sample in order to have a better sensitivity. A Rochar A 1439 frequencemeter is used for the frequency measurements. Two translation shutters allow to obtain the following exposures: 1) oscillating quartz only,

2) oscillating quartz and prism,

3) oscillating quartz, reference substrate and prism.

In general, we used one crucible to deposit the first film, about 500 Å thick, and the other for the evaporation of very thin superficial layers (< 50 Å). The oscillating quartz is calibrated

for each crucible by accurate measurements of thin film thickness by X-ray interferometry. Fig. 1 shows a schematic view of the vacuum chamber.

b) We can measure the sample resistance by a 4 point method. The electrical set-up for the resistivity measurements consists of a d.c. source and a resistance very much larger than the resistance of the sample, in order to create a constant current source. The intensity across the circuit is determined by the measurements of the voltage across a calibrated resistance. Generally, we regulate the intensity to 1 mA and, as the resistance of the thin film is a few ohms only, we have to measure potentials of the order of a few millivolts at the sample ends. A 148 Keithley nanovoltmeter is used for the voltage measurements. This instrument is provided with a zero shift, which allows sensitive measurements of the modifications of the sample resistance due to surface layers. One of the wires carrying the current is in Pd instead of Au, which makes a thermocouple allowing to measure the sample temperature. During the temperature determination, the resistivity measurements are interrupted.

As an example, fig. 2 shows the resistance modification ΔR of a silver film 250 Å thick when Pd is deposited on the free silver surface at room temperature. The deposition rate of Pd was about 2Å/minute and the resistance of the bare silver film was R_o = 1.05 ohm (20 x 24 mm substrate). The modifications of the film resistivity are mainly due to the modification of the conduction electron scattering at the surface. This technique can give

information on the adsorption phenomena {1}{2}. With this technique associated to Auger spectroscopy, we hope to obtain complementary results about the structure of the surface layer.

c) We can measure the reflection coefficient of the thin film sample deposited on the prism basis for polarized light and for angles of incidence between 15 and 70 degrees either from the prism side (frustrated total reflection) or from the vacuum side.

Fig. 3 shows the experimental set-up for the optical measurements as well as a schematic diagram of the electronics.

The source is a Osram 250 W quartz-halogen lamp working in the 0.4-2 μ spectral region. A 75 W Xenon arc lamp will be added in order to extend the measurements into the near ultra-violet.

We use a Coderg monochromator with a 1800 lines/mm grating blazed to 5000 Å and usable in the 3000-9000 Å wavelength region. The different orders are eliminated with color filters. The monochromator feed provides TTL pulses used to monitor the recorder.

The polarizer is a Glan-Thomson prism cemented for the ultra-violet.

The beam splitter was made by MTO Achrovex, giving $R \sim T \sim 0.3$ between 0.2 and 2 μ.

The photomultiplier is a Hamamatsu R777-01 model with a spectral response extending from 1850 to 9300 Å.

The electronics consist in a standard Ithaco (model 353A) system. The reference beam and the sample beam are modulated by a light beam chopper with a blade having two concentric sets of 19 and 20 apertures. The working frequency is about 1000 Hz. The detector output signal is amplified by an a.c. amplifier, the gain of which is controlled by an operational amplifier in order to obtain a constant output value (1 V) of the lock-in amplifier working at the reference beam frequency. The other lock-in amplifier gives the reflection coefficient value. A detailed description can be found in the Ithaco Application Note I.A.N.-31. All the mechanical components are standard Microcontrole units. All the external components are mounted on an optical table and can be aligned by three screws with the optical components which are inside the vacuum chamber.

The prism and the mirror inside the vacuum chamber are mounted on a goniometer which rotates with great precision ($\sim 0.01°$).

The crystallographic structure of the sample is controlled with a Philips electron microscope in service in our University, essentially by two techniques: transmission micrography of the films and analysis of carbon replicas of the sample surface. For very thin ($\sim$ 10 Å) and discontinuous surface layers deposited

on thicker films ($\sim$ 500 Å) (as in our experiments with gold on silver), it is possible to observe the island structure directly because the island dimensions are larger than the microscope resolution.

On the other hand, a very precise (1%) determination of the film thickness can be obtained by X-ray interferometry at grazing incidence (Kiessig method). This determination is used for the oscillating quartz calibration.

2. Description and analysis of optical data

2.1 General comments

With the experimental set-up which has been described, we can record the square of the reflection coefficient R^2 as a function of the wavelength for a given incidence Ψ. A recording of R^2 vs the angle of incidence for a given wavelength λ is also possible, but this has not been performed here.

From a physical point of view, in the first case(fixed Ψ and variable λ) the positions of the minima of the $R_p(\lambda)$ curves give the dispersion relation $\omega(K)$ of the surface plasma waves (S.P.) with real values of the reduced wave-vector $S = n_o \sin\Psi = K/K_o$ ($K_o = \omega/c$, n_o = prism refractive index) and complex values of the frequency $\omega = \omega_1 - i\omega_2$. The width of the resonance is related

in this case to the life-time of the wave-packet in the dispersive media. Alternatively, the angular positions of the minima of $R_p(\Psi)$ vs ω give the dispersion relation for real values of ω and complex values of $S = S_1 + iS_2$. In this case, the width of the resonance is related to the decay length of the wave-packet.

To excite SP we employ the ATR method in the Kretschmann configuration {3}. The thin metal film is about 500 Å thick and the thickness of this film is accurately determined by X-ray interferometry (Kiessig method); it can also be deduced from the optical data by fitting the values of R_p in the neighbourhood of the $R_p(\Psi)$ resonances. Fig. 4 shows the values of the film thickness deduced from the optical data for various λ ; the thickness determined by the Kiessig method is also indicated. The discrepancy between the two methods may be due to optical errors like beam divergence, etc... {3}. It must however be emphasized that the values deduced from optical data are remarkably constant for all wavelengths.

We are interested in the modifications produced at the surface by very thin surface layers, which we try to represent by a local dielectric constant $\varepsilon(\omega)$; therefore, we need the curves $R_p(\Psi)$ for many values of λ . This can be obtained by picking-up the values of R_p for each λ on the different recordings corresponding to a fixed incidence.

On the other hand, we can change the polarization of the light

and, in the spectral region where the SP cannot be excited, we can measure $R_p(\lambda)$ and $R_s(\lambda)$ for a given incidence from the vacuum side. We can also determine in this way the effect of a very thin surface layer, via $\Delta R_p/R_p$ and $\Delta R_s/R_s$.

2.2. Modifications of the resonance due to surface layers

In the last technical report (DA-ERO-75-G-02), we have stressed the effect of a very thin surface film (dielectric constant $\varepsilon_f = \varepsilon_{f1} - i\,\varepsilon_{f2}$, thickness d_f) on the SP propagation. We have shown that the resonance is modified in the following way:

a) A shift of the angular (frequency) position of the resonance, depending mainly on the relative values of the real parts of the dielectric constant of the surface layer ε_{f1} and of the substrate film ε_1;

b) A broadening of the resonance, very strongly dependent on the surface film absorption.

We have also established that, in the first order approximation in d_f/λ, the SP wave-vector for a bare surface K is modified into $K + \Delta K_f$ where

$$(1) \qquad \Delta K_f = K^2 \cdot \frac{(-\varepsilon)^{1/2}}{1-\varepsilon} \left[1 - \left(\frac{K}{K_0}\right)^2 \left(\frac{1}{\varepsilon_f} + \frac{\varepsilon_f}{\varepsilon}\right)\right] d_f$$

where $\varepsilon = \varepsilon_1 - i\varepsilon_2$ is the dielectric constant of the substrate film.

It must be underlined that, when $\varepsilon_{f2} \sim 0$ and ε_{f1} approaches zero or tends towards infinity, ΔK_f has a resonant behavior and becomes very large. This situation occurs when the surface layer material is a metal near its plasma frequency or a ionic crystal near its transverse optical phonon frequency ω_{TO} . In fact, in this case, equation (1) is no longer a good approximation. We present as an appendix a theoretical discussion of this particular case, which was published in Optics Communications (17, 342, 1976). Fig. 5 shows a recording of R_p^2 versus the wavelength for a thin silver film (568 Å thick) and for the same silver film covered by very thin gold deposits: 13, 25 and 30 Å thick. The absolute values of R_p are obtained when reported to a reference line nearly constant in this spectral region. We notice that the surface layers induce a shift and a broadening of the resonance. According to eq. (1), if the gold deposits have the same dielectric constant for every frequency, then for a given wavelength λ, ΔK_f is proportional to d_f. ΔK_f, being a small quantity, is proportional to the displacement of the angular position of the resonance for the given wavelength. The horizontal distances between the curves (1) and (2) and (1) and (3) are in the ratio 10/25, which shows that indeed ε_f has practically the same value for the Au films 10 and 25 Å thick. The spectral region covered by these experiments corresponds to the onset of the interband transitions in Au. Thus we are led to the conclusion that the strength and positions of the interband transitions in the metal are insensitive to the structure of the films and are essentially dominated by the local environment of the atoms.

Fig. 6 shows the values of R_p plotted versus the internal angle of incidence Ψ for λ = 4563 Å for the same experimental situation as in fig. 5. The minimum of the $R_p(\Psi)$ curves is shifted to greater angles of incidence by the Au deposits, that is to say to greater values of S_1; it is then clearly apparent that $\Delta S_1 > 0$. Formally, we have the same situation as a depletion layer in a semiconductor. The sign of ΔS_1 is essentially related to the relative values of the real parts of the substrate and surface layer dielectric constants: in this case $\varepsilon_1 = -1.2$ for gold and $\varepsilon_1 = -8.5$ for silver.

Fig. 7 corresponds to a $R_p(\Psi)$ resonance for a gold film (930 Å thick), modified by very thin deposits of silver, 6 and 14 Å thick. In this case, the gold film was too thick and the resonance is rather smeared out, but here again one can see the shift of the resonance; in this case it is towards smaller angles of incidence: that is to say : $\Delta S_1 < 0$. This situation is similar to an accumulation layer in semiconductors.

In fig. 8 we have plotted, versus the angle of incidence Ψ, the wavelengths of the minima of the $R_p(\lambda)$ curves for the free silver film surface and for silver covered by gold deposits 10 and 25 Å thick. The dispersion relation obtained in this way is not the same as the one corresponding to two infinite media, that is to say $K = \omega/c\ (\varepsilon/\varepsilon+1)^{1/2}$ because, in our experiments as well as in all ATR experiments, one must take into account the effect of the finite thickness of the film (or prism-metal surface

distance). For thick enough films, this discrepancy is not very important.

2.3. Determination of the surface layer optical constants

A simple inspection of the resonance shapes can often give information about the optical behavior of the surface layer material; for instance, if the resonances are only shifted we can say that the material is not absorbing ($\varepsilon_{f2} = 0$).

More generally, we can determine ΔK_{f1} and ΔK_{f2} and then, if we know the surface layer thickness d_f and the substrate dielectric constant ε, we can go a step forward and compute the surface layer optical constants.

In this paragraph, we shall analyse the possible solutions which can be obtained for ε_f from the values of ΔK_f in a model of continuous and homogeneous layer. This simple model is not valid if the surface layer is discontinuous or if the surface layer modifies very strongly the surface electronic properties of the substrate. Such a case is much more typical of semiconductors than of metals.

In fig. 9 and fig. 10, we have drawn in the $(\varepsilon_{f1}, \varepsilon_{f2})$ plane the curves : $\alpha_1 = \Delta S_1 / (2\pi d_f/\lambda)$ = constant and $\alpha_2 = \Delta S_2 / (2\pi d_f/\lambda)$ = constant for an arbitrary value of $\varepsilon = -10 - i0$ where $\Delta S_1 = \Delta K_{f1} / K_0$ and $\Delta S_2 = \Delta K_{f2} / K_0$

These quantities were computed from equation(1). In the α_1 - plot (fig. 9), we notice that, for a given value of α_1, there are always both an open branch and a closed branch, one in the $\varepsilon_{f1} > 0$ half-plane, the other one in the $\varepsilon_{f1} < 0$ half-plane. The full line corresponds to the values $\alpha_1 = 0$ and it represents a boundary between the regions where ΔK_{f1} has positive and negative values. Here again, the region $\varepsilon_f \sim 0$ has no physical meaning, because in this region eq. (1) is not valid. When $\varepsilon_2 = 0$, the α_2-plot is completely symmetric (fig. 10), that is to say $\alpha_2(\varepsilon_{f1}) = \alpha_2(-\varepsilon_{f1})$ as it can be deduced fom eq. (1).

The ε_f values for a given set of α_1 and α_2 are obtained by the intersection of such lines. There are always two solutions, one for which $\varepsilon_{f1} > 0$ and the other with $\varepsilon_{f1} < 0$; in general, it is a straightforward matter to choose the solution with physical meaning.

The α_1 = const. and α_2 = const. curves depend on the ε_2 values. Fig. 11 and fig. 12 correspond to $\varepsilon = -10 - i1$, which are typical values for silver in the visible region. We find that the α_1 and α_2 curves are distorted, but they retain the same general shape. It must be emphasized that α_2 can take negative values if the absorption in the surface layer is smaller than in the substrate.

An important point, clearly apparent from these figures, is that the α_1 and α_2 curves intersect nearly orthogonally, showing

that an accurate determination of ε_f can be expected. We also notice that an error on ΔS_1 leads to an error mainly on ε_{f1} and, alternatively, an error on ΔS_2 leads to an error on ε_{f2}.

2.4. Comparison with differential reflection spectroscopy

In the past, only ellipsometry was used for optical studies of surface layers but with the increasing interest in surface studies, other techniques appeared. Differential reflection spectroscopy is one of the most popular techniques for the investigation of very thin films in the submonolayer range {4}. A formula first derived by J.D.E. McIntyre and D.E. Aspnes {5}, and correct to the first order in d_f/λ, seems to be a good approximation for most of the practical cases. In our notation, $\varepsilon_f = \varepsilon_{f1} - i\,\varepsilon_{f2}$ for the surface layer and $\varepsilon = \varepsilon_1 - i\,\varepsilon_2$ for the substrate, one can write for s-polarized light:

$$(2) \qquad \frac{\Delta R_s}{R_s} = \frac{8\pi d_f \cos\varphi}{\lambda}\, \mathrm{Im}\left(\frac{\varepsilon_f - \varepsilon}{1-\varepsilon}\right)$$

and for p-polarized light:

$$(3) \qquad \frac{\Delta R_p}{R_p} = \frac{8\pi d_f \cos\varphi}{\lambda}\, \mathrm{Im}\left\{\left(\frac{\varepsilon_f - \varepsilon}{1-\varepsilon}\right)\left(\frac{1-(1/\varepsilon\varepsilon_f)(\varepsilon+\varepsilon_f)\sin^2\varphi}{1-(1/\varepsilon)(1+\varepsilon)\sin^2\varphi}\right)\right\}$$

These formulas are similar to the Drude formula for the ellipsometric quantities Ψ and Δ.

We did not determine directly the $\Delta R/R$ values, but we measured

the absolute values of R and ΔR for s- and p-polarized light for silver films on gold in the 4000-6000 Å spectral range for an incidence $\varphi = 60°$. We will discuss here the possibilities of obtaining ε_f from $\Delta R_p/R_p$ and $\Delta R_s/R_s$ for a given angle of incidence.

D.M. Kolb and J.D.E. McIntyre have shown {6} that in this first order approximation:

$$\varepsilon_{f2} = a_1 - a_2 \cdot \varepsilon_{f1}$$

Where:

$$a_1 = \frac{1}{1-\varepsilon_1}\left[\varepsilon_2 - \left\{(1-\varepsilon_1)^2 + \varepsilon_2^2\right\} \cdot \frac{\Delta R_s/R_s}{2\pi\cos\varphi\,(d_f/\lambda)}\right]$$

$$a_2 = \frac{\varepsilon_2}{1-\varepsilon_1}$$

For comparison with fig. 9-12, we have plotted in fig. 13 $\gamma_1 = (\Delta R_s/R_s)/(2\pi d_f/\lambda)$ = constant in the $(\varepsilon_{f1}, \varepsilon_{f2})$ plane; $\varepsilon = -10+i1$ as in fig. 11 and 12. These curves are always straight lines; the ε_{f2}-axis intersection a_1 depends on ε and the $\Delta R_s/R_s$ values, but the slope a_2 is dependent on the substrate optical constants only.

For p-polarized light, we have {6}:

$$\beta_1 \varepsilon_{f1} + \beta_2 \varepsilon_{f2} + \frac{\beta_3 \varepsilon_{f1} + \beta_4 \varepsilon_{f2}}{\varepsilon_{f1}^2 + \varepsilon_{f2}^2} + \beta_5 = 0$$

Where

$$\beta_1 = \nu\varepsilon_2\left(\varepsilon_1^2 + \varepsilon_2^2 - 2u\varepsilon_1\right)$$

$$\beta_2 = \nu(1-\varepsilon_1)\left(\varepsilon_1^2 + \varepsilon_2^2 - 2u\varepsilon_1\right) + u^2\left[(1-\varepsilon_1)^2 + \varepsilon_2^2\right]$$

$$\beta_3 = u\varepsilon_2(\varepsilon_1^2 + \varepsilon_2^2 - 2u\varepsilon_1)$$

$$\beta_4 = u\left\{(\varepsilon_1^2+\varepsilon_2^2)\left[v(\varepsilon_1^2+\varepsilon_2^2) - \varepsilon_1\right] + u(\varepsilon_1^2 - \varepsilon_2^2)\right\}$$

$$\beta_5 = \frac{(\Delta R_p/R_p)}{8\pi\cos\Psi(d_f/\lambda)}\left[(1-\varepsilon_1)^2+\varepsilon_2^2\right]\left[(u-v\varepsilon_1)^2+v^2\varepsilon_2^2\right] - \varepsilon_2(\varepsilon_1^2+\varepsilon_2^2-2u\varepsilon_1)$$

and

$$u = \sin^2\Psi \quad , \quad v = \cos^2\Psi \ .$$

In fig. 14, we have plotted ε_{f2} vs ε_{f1} curves for $\gamma_2 = cst$ ($\varepsilon = -10 - i1$, $\Psi = 70°$). We see that solutions for ε_f cannot be determined with accuracy, at least for large absolute values of ε_f (as it is the case for metals). On the contrary, for highly reflecting substrates, the SP method works very well. From this point of view, the two methods are complementary.

Fig. 15 and 16 show γ_1 and γ_2 plots for a rather different case: a highly absorbing substrate ε = -1-i6 and Ψ = 60° (we have chosen Ψ = 60° because this is the angle used in one of our experiments). We see that the slopes of the γ_1 = const. and γ_2 = const. curves are different enough for a precise determination of their intersection points.

A point which must not be forgotten is that the precision in the determination of ε_f does not depend on the magnitude of the experimental quantities only. For instance, in fig. 11 and 12, one notices that for $\varepsilon_f \sim \varepsilon_1$ the values of ΔK_1 and ΔK_2 are very small, notwithstanding an accurate determination of ε_f can still be obtained.

3. Experimental results

3.1 Gold on silver

a) Crystallographic structure

A few years ago, J.P. Allpress and J.V. Sanders {7}, studying decoration of facets on silver, found that gold condenses on simple facets as a discontinuous deposit with randomly distributed islands. For the complex facets, the deposits are much more continuous.

As we have already indicated, our films have a (1,1,1) preferential orientation, and we can expect island formation for gold deposits.

Fig. 18 shows a carbon replica of the sample surface for a gold deposit, 17 Å thick. This C-replica was obtained after the sample had been immersed in a HNO_3 solution in which only Ag was attacked. The island diameter is about 60 Å, with a density of $4.10^{11}/cm^2$, and we conclude that the island thickness is of the order of their lateral dimensions. In this picture, we can also see the prints of the grain boundaries limiting the microcrystals in the Ag substrate. Of course, electron microscope investigations cannot provide information about surface growth at the very beginning of Au deposition.

b) Optical constants

Using the exact electromagnetic formula for multilayer systems {8}, we have computed the ε_f values as a function of λ with a least square fitting program (from the Health Sciences Computing Facility UCLA). We have chosen experimental points in the neighborhood of the resonance, where the effect of a surface layer is most important. We compute first the substrate optical constants ε (silver in these experiments) and the film thickness (see fig. 5), and these values are used for a later calculation of ε_f .

Fig. 19 shows the values of ε_{f1} and ε_{f2} between 4000 and 6000 Å for thin layers of Au on Ag with d_f = 13 and 27 Å. It is found that the values of ε_{f1} over the whole spectral range are independent of d_f, negative and very close to the optical constants determined by accurate measurements on well-crystallized thicker Au films {9}. We have an analogous situation for ε_{f2}; nevertheless the errors are more important (they are essentially related to errors on ΔK_2). It must be emphasized that the absolute values of ε_f may depend appreciably on the values chosen for d_f but the general shape of the curve remains the same. In any case, we find ε_f values close to the bulk values within our experimental uncertainties for layer thicknesses from 10 to 40 Å.

It is easy to estimate that for islands of about 60 Å, about 1/3 or 1/4 of their atoms lay at the surface, and we expect

important surface effects. For very small thicknesses, no conclusio can be derived from our experiments. But for larger thicknesses, the observation that ε_f equals the bulk values for very discontinuous layers with island dimensions of the order of 200 Å suggests that the model of a continuous layer is valid in all cases and that roughness effects are not very important.

3.2. Silver on gold

a) Crystallographic structure

We do not know the crystallographic structure of gold deposits on silver. Electron microscope investigations did not give any information (for d_f = 14 Å) and we suppose therefore that the deposits are much more continuous than in the gold/silver system. Electron diffraction is not useful because the Au and the Ag lattice parameters are very close (4.078 Å for Au and 4.085 Å for Ag). To our knowledge, only C. Pariset has studied this system by resistivity measurements and X-ray diffraction{10}. He found that, at room temperature, silver grows on (1,1,1) gold according to a bidimensional structure and probably in epitaxy with the substrate as they deduce from X-ray diffraction experiments on gold-silver-gold sandwiches.

b) Optical constants

The spectral range where the SP method can be used in this

case is not very large because in gold, for wave lengths shorter than about 5500 Å, there are important d $\rightarrow$ s-p interband transitions and free electron excitations as surface plasmons cannot take place anymore.

Fig. 19 shows the optical constants of silver deposits (6 and 14 Å) on gold in the narrow spectral range 5500-6000 Å. The continuous line corresponds to the optical constants determined by accurate measurements on well-crystallized thicker Ag films {11}.

It is found that ε_{f1} is more negative than the bulk values and that the shape of the $\varepsilon_{f1}(\lambda)$ curve changes with d_f. $\varepsilon_{f2}(\lambda)$ has a behavior very different from the nearly constant values of bulk optical constants. For increasing thickness, we approach the values corresponding to thick layers.

From the vacuum side, for an angle of incidence of $\Psi = 60°$, we have measured R_p^2 and R_s^2 for the bare gold surface and for silver (d_f = 6,14 Å) deposited on gold and we have then deduced the relative variations of these two quantities. We have also computed the theoretical values of $\Delta R_p/R_p$ and $\Delta R_s/R_s$ deduced from the optical constants for gold {9} and silver {11} and the exact formula for multilayer systems. As explained before, in our experiments, we measure the absolute values of the reflection coefficients in each case and in our experimental situation we have important errors for small values of R. Fig. 20 shows the

experimental values of $\Delta R_p/R_p$ together with the errors estimated from producibility of the measurements. We see that in the absorbing region the R_p/R_p errors are very important while in the reflecting region, we have already shown (section 2.4,fig. 13 and 14) that this method is not appropriate to determine the surface layer optical constants.

Fig. 20 shows R_s/R_s for the same situation as in fig. 19. The gold film was 930 Å thick and can be considered as a infinite medium.

From the exactly computed curves as well as from the approximate equations (2) and (3), we see that the ratio $(R/R)_{df=14}/(R/R)_{df=6}$ is equal to 14/6. This is also more or less what we observed in our experiments between 4000 and 5000 Å, but not at all in the 5000-6000 region. The discrepancy between the experimental and the theoretical curves is also more important in this region. On the other hand it is precisely here that we obtained $f1$ and $f2$ with the SP method and these values are different from the bulk values.

Conclusion

In paragraph 3, we have demonstrated on two examples (silver on gold and gold on silver) the practical possibilities of the SP optical spectroscopy. We have shown that it can be employed in the

submonolayer range and that it allows to determine the effective dielectric constants of the surface layer.

This method can only be used with highly reflecting metals: it is precisely in this case that the other methods prove to be quite insensitive to surface phenomena. It appears that it would be very interesting to study very small surface coverage using differential reflection measurements in the SP configuration.

Now we hope to investigate systems in which the surface deposit in the very small thickness range is much more continuous than in the cases studied here.

References

{1} J.W. Geus, Chemisorption and Reaction on Metallic Films, Academic Press (1971).

{2} C. Pariset, J.P. Chauvineau, Surf. Sci. 47, 154 (1975). C. Pariset, Galtier, Gasnier, Thin Solid Films 29, 325 (1975).

{3} E.Kretschmann, Z. Physik 241, 313 (1971).

{4} J.D.E. McIntyre in Opt. Prop. of Solids, ed. by B.O. Seraphin, North-Holland (1976), p. 555.

{5} J.D.E. McIntyre and D.E. Aspnes, Surf. Sci. 24, 417 (1971).

{6} D.M. Kolb and J.D.E. McIntyre, Suf. Sci. 28, 321 (1971).

{7} J.G. Allpress and J.V. Sanders, Fil. Mag. 9, 645 (1964).

{8} F. Abelès, in "Advanced Optical Techniques", edited by A.C.S. van Hell, North-Holland Publishing Co., Amsterdam p.144 (1967).

{9} M.L. Thèye, Phys. Rev. B2, 3060 (1970).

{10} C. Pariset, Thesis, Orsay, France (1976).

{11} M.M. Dujardin and M.L. Thèye, J. Phys. Chem. Solds 32, 2033 (1971).

Figure Captions

Figure 1: Schematic view of the vacuum chamber. P prism (sample), M mirror, RS reference sample, sh shutter, c crucibles SV slide valve, Ti.S.P. sublimation pump, N_2P liquid N_2 trap, Ip ionic pump.

Figure 2: Modification of the resistance (R_o = 1) of a silver thin film as a function of the variation of the frequency of the oscillating quartz during the condensation of Pd at the silver surface at the rate of 30 Hz/minute (15 Hz $\approx$ 1Å of Pd).

Figure 3: Schematic diagram of the optical and electronic experimental set-up. M monochromator, P polarizer, sh shutter PM photomultiplier.

Figure 4: Thin film thickness as determined from the $R_p^2(\varphi)$ resonances for different values of the wavelength λ

Figure 5: R_p^2 vs λ (arbitrary units) for a silver film (658 Å thick) and for thin gold layers of mass thickness 10,25 and 30 Å deposited on the free silver surface. The internal angle of incidence was $\varphi \simeq 46.5°$.

Figure 6: R_p vs φ for the same experimental situation as in fig. 1.

Figure 7: Values of R_p vs the internal angle of incidence φ for a Au film (^{p}(930 Å thick), for thin silver layers of mass thickness 6 Å and 1[illegible] Å deposited on the free Au surface λ = 5818 Å.

Figure 8: Values of λ corresponding to the minimum in the $R_p(\lambda)$ curves vs the internal angle of incidence φ for a^p silver thin film (655 Å thick), bare and covered by 10 and 25 Å of gold. The prism refractive index is n_p = 1.476 for λ = 4000 and n_p = 1.464 for 6000 Å.

Figure 9: Isovalues of $\Delta S_1/(2\pi d_f/\lambda)$ plotted in the $\varepsilon_{f1} - \varepsilon_{f2}$ plane according to formula (1). The substrate dielectric constant was chosen equal to ε = -10-i0.

Figure 10: Isovalues of $\Delta S_2/(2\pi d_f/\lambda)$ in the same conditions as in fig. 9.

Figure 11: Isovalues of $\Delta S_1/(2\pi d_f/\lambda)$. ε substrate = -10-i1.

Figure 12: Isovalues of $\Delta S_2/(2\pi d_f/\lambda)$. ε substrate = -10-i1.

Figure 13: Isovalues of $(\Delta R_s/R_s)/(2\pi d_f/\lambda)$ in the $\varepsilon_{f1} - \varepsilon_{f2}$ plane computed according to formula (2) for the angle of incidence φ = 70° and ε substrate = -10-i1.

Figure 14: Isovalues of $(\Delta R_p/R_p)/(2\pi d_f/\lambda)$ in the $\varepsilon_{f1}-\varepsilon_{f2}$ plane computed according to formula (3) in the same conditions as in fig. 13.

Figure 15: Isovalues of $(\Delta R_s/R_s)/(2\pi d_f/\lambda)$ in the $\varepsilon_{f1}-\varepsilon_{f2}$ plane for φ = 60° and ε substrate = -1-i6.

Figure 16: Isovalues of $(\Delta R_p/R_p)/(2\pi d_f/\lambda)$ in the same conditions as in fig. 15.

Figure 17: Carbon replica of a silver surface covered by 17 Å of gold. The small black points correspond to the gold microcrystals.

Figure 18: Values of ε_{f1} and ε_{f2} for gold surface layers (13 and 27 Å thick) deposited on free silver surface. The continuous line corresponds to the bulk values for Au taken from ref. 9 .

Figure 19: Values of ε_{f1} and ε_{f2} for silver surface layers (6 and 14 Å thick) deposited on free gold surface. The continuous line corresponds to the bulk values for Ag taken from ref. 11 .

Figure 20: $(\Delta R_p/R_p)$ for silver surface layers (6 and 14 Å thick) deposited on the free surface of a gold film (930 Å thick). The angle of incidence was φ = 60°. The continuous line was computed with values taken from ref. 9 and 11 .

Figure 21: $(\Delta R_s/R_s)$ for the same experimental situation as in Fig. 20.

Appendix

MODIFICATION OF THE DISPERSION RELATIONS FOR SURFACE PLASMONS BY VERY THIN SURFACE FILMS IN THE VICINITY OF THEIR PLASMA FREQUENCY

T. LOPEZ-RIOS
Laboratoire d'Optique des Solides, Université Paris VI, 4 Place Jussieu, 75230 Paris Cedex 05, France*

Received 1 February 1976

Dispersion curves are calculated for a situation corresponding to a very thin K film on Al. The vicinity of the plasma frequency of the film is thoroughly investigated and the influence of absorption in the film is stressed. The gap in the dispersion curve computed at constant frequency disappears with increasing absorption in the film. Experimental possibilities for investigating very thin films by ATR are discussed and an approximate expression for the predicted splitting of the minimum of the reflectance for p-polarized light is given. The splitting is shown to be independent of the absorption in the film.

1. Introduction

The dispersion relations for surface polaritons [1, 2] and surface plasmons (SP) [3] have already been discussed by several authors, even for multilayer systems. We shall discuss here the situation where a very thin metal film is supported by a metallic substrate propagating surface waves at its interface with vacuum or a dielectric. The modification of the surface waves due to the alteration of the metal surface can provide information about surface phenomena like chemisorption, metallic adsorption or oxidation.

In the general case, the presence of a very thin film (thickness $d_f \ll$ wavelength λ) at the metal–dielectric interface leads to a shift of the dispersion curve (frequency ω versus k, the projection of the wavevector along the interface) and a broadening related to the absorption of the film. The analysis of the influence of the film can be performed by using a first order approximation (linear in $k_0 d_f$, with $k_0 = \omega/c$), therefore the modifications of k are proportional to the film thickness. This approximation breaks down when $k/k_0 \gg 1$ and $(k/k_0)k_0 d_f$ is no more a small quantity. Such a situation is not encountered in optical experiments using the SP excitation by attenuated total reflection (ATR) [4,5]. The linear approximation has already been used for the investigation of surface [6] and interface [7] modifications.

Another case where the first-order approximation may be questioned, corresponds to the frequencies for which the dielectric function of the film (ϵ_f) goes to zero or to infinity. For ionic crystals, this occurs at ω_{LO} and ω_{TO} (longitudinal and transverse optical phonon frequencies) respectively. This situation has been discussed by Agranovich et al. [8] and it leads to a splitting of the surface polaritons. Experimental evidence for this has been provided by Yakovlev et al. [9] who have investigated LiF films on sapphire (Al_2O_3) and rutile (TiO_2). For metals, this occurs at the plasma frequency ω_p. Economou et al. [3] have discussed the dispersion curve corresponding to a metal film on a metal substrate, but only for the case corresponding to real values of k.

We present here an analysis for the same situation (metal film on metal substrate), but we discuss important effects due to the damping (absorption) in the film. In addition, we investigate both real and complex values of k, pointing out the differences observed in experiments conducted either at fixed k/k_0 and variable ω or at fixed ω and variable k/k_0, and we present curves showing the expected behavior of the reflectance for p-polarized light (R_p) measured at

* Equipe de Recherche Associée au C.N.R.S.

fixed incidence and variable ω in an ATR configuration. The computations were performed in the case of a K film on Al. They do not take into account possible (and probable) spatial dispersion effects.

2. Dispersion relations

Let $\epsilon = \epsilon_1 - i\epsilon_2$ and ϵ_0 be the dielectric functions of a metallic plasma and of a dielectric, which are in contact. The condition for occurrence and propagation of an SP at the ϵ/ϵ_0 interface is given by $Z + Z_0 = 0$, where Z and Z_0 are the optical admittances of a p-polarized wave in both media, with $Z = \epsilon \times (\epsilon - S^2)^{-1/2}$ and $Z_0 = \epsilon_0(\epsilon_0 - S^2)^{-1/2}$ and $S = k/k_0$. It is well known [1] that this condition leads to the dispersion relation

$$S^2 = (k/k_0)^2 = \epsilon\epsilon_0/(\epsilon + \epsilon_0) \qquad (1)$$

where ϵ is a function of ω and ϵ_0 is assumed to be frequency independent.

The presence of a thin film at the ϵ/ϵ_0 interface leads to a modified condition for the occurrence and propagation of SP, namely [10,11]

$$Z + Z_0 + (ZZ_0/Z_f + Z_f)\tanh\varphi = 0, \qquad (2)$$

with $Z_f = \epsilon_f(\epsilon_f - S^2)^{-1/2}$ and $\phi = k_0 d_f(S^2 - \epsilon_f)^{1/2}$. SP can be excited by working either at fixed frequency and variable S or at fixed S and variable frequency. It has been shown by Alexander et al. [12] that the dispersion curves obtained at the ϵ/ϵ_0 interface in these two cases coincide only when $\epsilon_2 = 0$. In order to show the effect of a very thin layer on SP in the vicinity of its plasma frequency $\omega_{pf} = 2\pi c/\lambda_{pf}$, we have chosen an example corresponding to a K film ($d_f = 20$ Å) on Al. The dielectric constants of the two metals are given by the Drude expressions:

$$\epsilon = 1 - \omega_p^2/\omega^2(1 - i/\omega\tau),$$

$$\epsilon_f = 1 - \omega_{pf}^2/\omega^2(1 - i/\omega\tau_f),$$

with $\lambda_p = 2\pi c/\omega_p = 837$ Å, $\hbar\omega_p = 14.88$ eV, $\omega_p\tau = 24.85$ for Al [13], $\lambda_{pf} = 3260$ Å, $\hbar\omega_{pf} = 3.80$ eV, for K [14] and different values of the relaxation time for the conduction electrons in the film: $\omega_{pf}\tau_f = 10$ and 50, τ_f being strongly dependent on the crystalline structure of the film. We explore the region of frequencies comprized between $0.8\omega_{pf}$ and $1.2\omega_{pf}$,

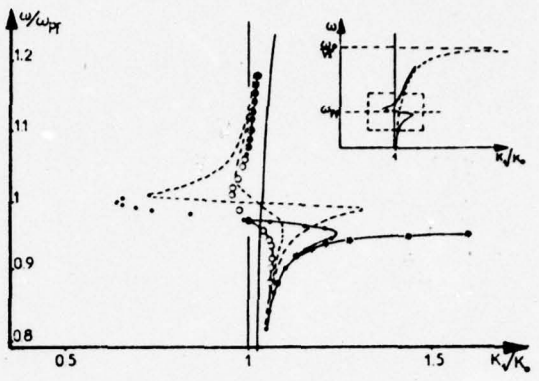

Fig. 1. ω/ω_{pf} versus k_1/k_0 obtained from eq. (2) (for ω real and k complex) for a K film ($d_f = 20$ Å, $\hbar\omega_{pf} = 3.80$ eV [14]) on Al ($\hbar\omega_p = 14.88$ eV, $\omega_p\tau = 24.85$ [13]). The open circles, the full circles and the stars correspond to $\omega_{pf}\tau_f = 10$, 50 and infinity, respectively. The dashed lines are computed in the linear approximation according to eq. (3). The full continuous line corresponds to a bare Al surface. The insert contains a schematic dispersion curve for frequencies up to $\omega_p/2^{1/2}$.

in which the influence of the surface layer ϵ_f is the most important.

Figs. 1 and 2 show the solution of eq. (2) for real values of ω and complex values of $S = k/k_0 = S_1 - iS_2 = (k_1 - ik_2)/k_0$. Fig. 1 displays the relation between ω and the real part of k/k_0, i.e. S_1. In our notation, the light line corresponds to $S_1 = 1$ and it is represented by a vertical straight line. The dispersion relation corresponding to bare Al in contact with vacuum (ϵ/ϵ_0 interface) is represented by a continuous line.

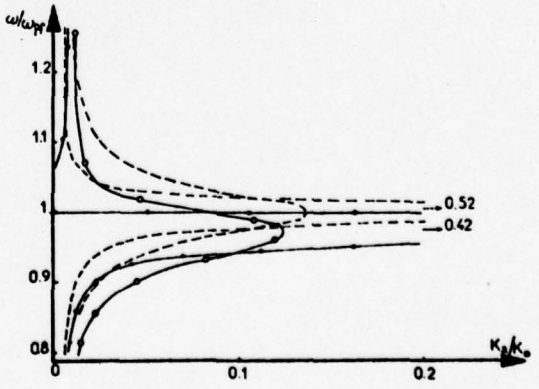

Fig. 2. ω/ω_{pf} versus k_2/k_0 for the same situations and with the same notations as in fig. 1.

It is a smooth curve close to the light line over the frequency range of interest: $0.8\omega_{pf}$ to $1.2\omega_{pf}$. The curves corresponding to the presence of a very thin K film are characterized by an important backbending which is strongly dependent on the absorption in the film (i.e. on the value of τ_f).

When $\epsilon_{f2} = 0$, there are two distinct branches going to the limit values $\omega = \omega_{pf}/2^{1/2}$ and $\omega = \{(\omega_p^2 + \omega_{pf}^2)/2\}^{1/2}$ corresponding to SP at the K–vacuum interface and at the Al–K interface respectively. When $\epsilon_{f2} \neq 0$, the dispersion curves show backbending. For large absorption, the two distinct branches are no longer observed and the curves are continuous. The dispersion curves have been drawn on both sides of the light-line $S_1 = 1$. For $S_1 > 1$ we have true SP, whereas for $S_1 < 1$ we do not have evanescent waves in the vacuum. This case is referred to in the literature [15] as leading to leaky Fano modes at the surface. For large damping in the surface layer (τ_f small), the whole dispersion curve is situated to the right of the light-line, that is $S_1 > 1$.

Fig. 2 displays the relation between ω and the imaginary part of k/k_0, i.e. S_2. Both curves corresponding to $\omega_{pf}\tau_f = 10$ and 50 show a maximum for $\omega \simeq \omega_{pf}$, the intensity of which decreases with increasing damping. As the propagation length of an SP along the surface, L, is related to S_2 through $L = \lambda/2\pi S_2$, it is clear that L reaches a minimum at $\omega \simeq \omega_{pf}$. It should be noticed that the curve with stars in fig. 1 also corresponds to the solutions of eq. (2) with real S and complex $\omega = \omega_1 + i\omega_2$, even when $\epsilon_{f2} \neq 0$ because these solutions are almost insensitive to absorption.

Another important point to be made is that for large values of τ_f (small absorption in the surface layer), there is a gap in the dispersion curve. In our case, this can be seen on the curves giving ω versus S_1 and ω versus S_2 (figs. 1 and 2) for $\omega_{pf}\tau_f = 50$. There is no gap for $\omega_{pf}\tau_f = 10$. There is nothing equivalent when solving eq. (2) for real S and complex ω.

These results can be understood, at least qualitatively, by looking for an approximate solution of eq. (2), corresponding to the approximation $\tanh\phi \approx \phi$. In this linear approximation one finds that, if k is given by eq. (1), then the solution of eq. (2) is given by $k + \delta k$ with [6,11]

$$\delta k = k^2 \frac{(-\epsilon_0\epsilon)^{1/2}}{\epsilon_0 - \epsilon}\left[1 - \left(\frac{k}{k_0}\right)^2\left(\frac{1}{\epsilon_f} + \frac{\epsilon_f}{\epsilon\epsilon_0}\right)\right] d_f. \qquad (3)$$

The dispersion curves computed according to eq. (3) are represented by dashed lines in figs. 1 and 2. They are similar to the curves computed exactly from eq. (2) and discussed above, the slight shift of their inflexion point (in fig. 1), or peak (in fig. 2) being due to a breakdown of the linear approximation in the immediate vicinity of ω_{pf}.

The optical excitation and detection of SP is usually performed using an ATR configuration. As stressed before, the experiments can be conducted either at fixed frequency and variable incidence or at fixed incidence and variable frequency. In the former case, it appears from fig. 1 that there is one and only one point on the dispersion curve which is reached for each frequency. When working at fixed incidence, that is to say at constant k/k_0, there are always two points on the dispersion curve which are reached for two different frequencies: the intersection of the line k/k_0 = const. with the dispersion curve in a ω_1 versus k/k_0 representation (this curve is identical to the curve with stars in fig. 1). In a first-order approximation, the distance between them has been given by Abelès [11]. In our case, with $\omega_p \gg \omega_{pf}$, its approximate expression is

$$\delta\lambda/\lambda_{pf} = \pm (\pi d_f/\lambda_p)^{1/2} \qquad (4)$$

which shows that even for very small thicknesses of the surface film, $\delta\lambda$ can be easily measured. Fig. 3 shows the computed curves for R_p versus λ in an ATR experiment at fixed incidence using the indicated con-

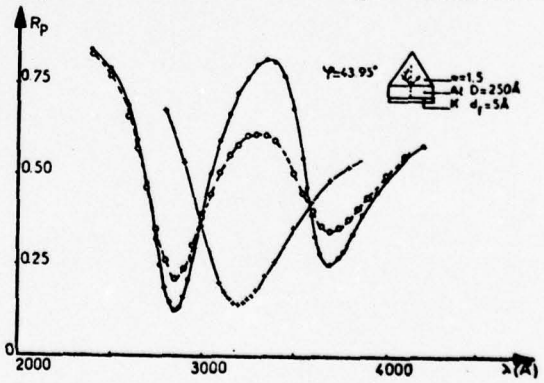

Fig. 3. Computed values of the reflectance for p-polarized light, R_p, in an ATR configuration schematically shown in the insert for an Al surface covered with a very thin K film (d_f = 5 Å) and for different values of the absorption in the film (open circles: $\omega_{pf}\tau_f = 10$, full circles: $\omega_{pf}\tau_f = 50$). The crosses give the values of R_p for a bare Al surface.

figuration. The values of λ corresponding to the minima of R_p give the positions of the points on the dispersion curve corresponding to the given incidence $\phi = 43°95$. The curve joining the crosses is for an Al–vacuum interface, the two other curves representing the effect of a very thin K film ($d_f = 5$ Å) on Al. The curves with full and open circles correspond to $\omega_{pf}\tau_f = 50$ and 10 respectively. It is apparent that the positions of the minima are not dependent on the absorption in the K film, which only causes a broadening of the resonance.

3. Conclusion

For a thin metal film on a metal substrate, we have discussed the influence of the absorption in the film on the SP dispersion curves. The presence of a gap in the curve computed for real ω and complex k is strongly dependent on the absorption in the film, the gap vanishing for strong absorption. It has been shown that for a very thin film of K on Al ($d_f = 5$ Å), a rather large (800 Å) splitting of the SP resonance in an ATR experiment conducted at fixed incidence takes place in the vicinity of the plasma frequency of the film, the resonance frequency being independent of the absorption (τ_f) in the film. An approximate expression allowing a rapid estimate of the splitting has been given. It is clear that films as thin as 1 Å ought to be easily detected by this method.

Acknowledgement

The author is indebted to Professor F. Abelès for advice and guidance during the performance of this work. The partial support of the European Research Office is gratefully acknowledged.

References

[1] E. Burstein, W.P. Chen, Y.J. Chen and A. Hartstein, J. Vac. Sci. Technol. 11 (1974) 1004.
[2] C.A. Ward, R.W. Alexander and R.J. Bell, Phys. Rev. B 12 (1975) 3293.
[3] E.N. Economou, Phys. Rev. 182 (1969) 539; K.L. Ngai and E.N. Economou, Phys. Rev. B 4 (1971) 3132.
[4] A. Otto, Z. Physik 216 (1968) 398.
[5] E. Kretschmann, Z. Physik 241 (1971) 313.
[6] F. Abelès and T. Lopez-Rios, in: Polaritons, Proc. 1st Taormina Res. Conf. Structure of Matter, ed. by E. Burstein and F. de Martini (Pergamon, New York, 1974) p. 241.
[7] F. Abelès, T. Lopez-Rios and A. Tadjeddine, Solid State Commun. 16 (1975) 843.
[8] V.M. Agranovich and A.G. Malshukov, Opt. Commun. 11 (1974) 169.
[9] V.A. Yakovlev, V.G. Nazin and G.N. Zhizhin, Opt. Commun. 15 (1975) 293.
[10] E.N. Economou and K.L. Ngai, in: Advances in Chemical Physics, ed. by I. Prigogine and Stuart A. Rice, p. 298.
[11] F. Abelès, Thin Solid Films, to be published.
[12] R.W. Alexander, G.S. Kovener and R.J. Bell, Phys. Rev. Lett. 32 (1974) 154.
[13] W.R. Hunter, J. Physique 25 (1964) 154.
[14] N.V. Smith, Phys. Rev. B 138 (1969) 634; J. Monin and G.A. Boutry, Phys. Rev. B 9 (1974) 1309.
[15] E. Burstein, A. Hartstein, J. Schoenwald, A.A. Maradudin, D.L. Mills and R.F. Wallis, in: Polaritons, Proc. 1st Taormina Res. Conf. Structure of Matter, ed. by E. Burstein and F. de Martini (Pergamon, New York, 1974) p. 241.

Fig 1

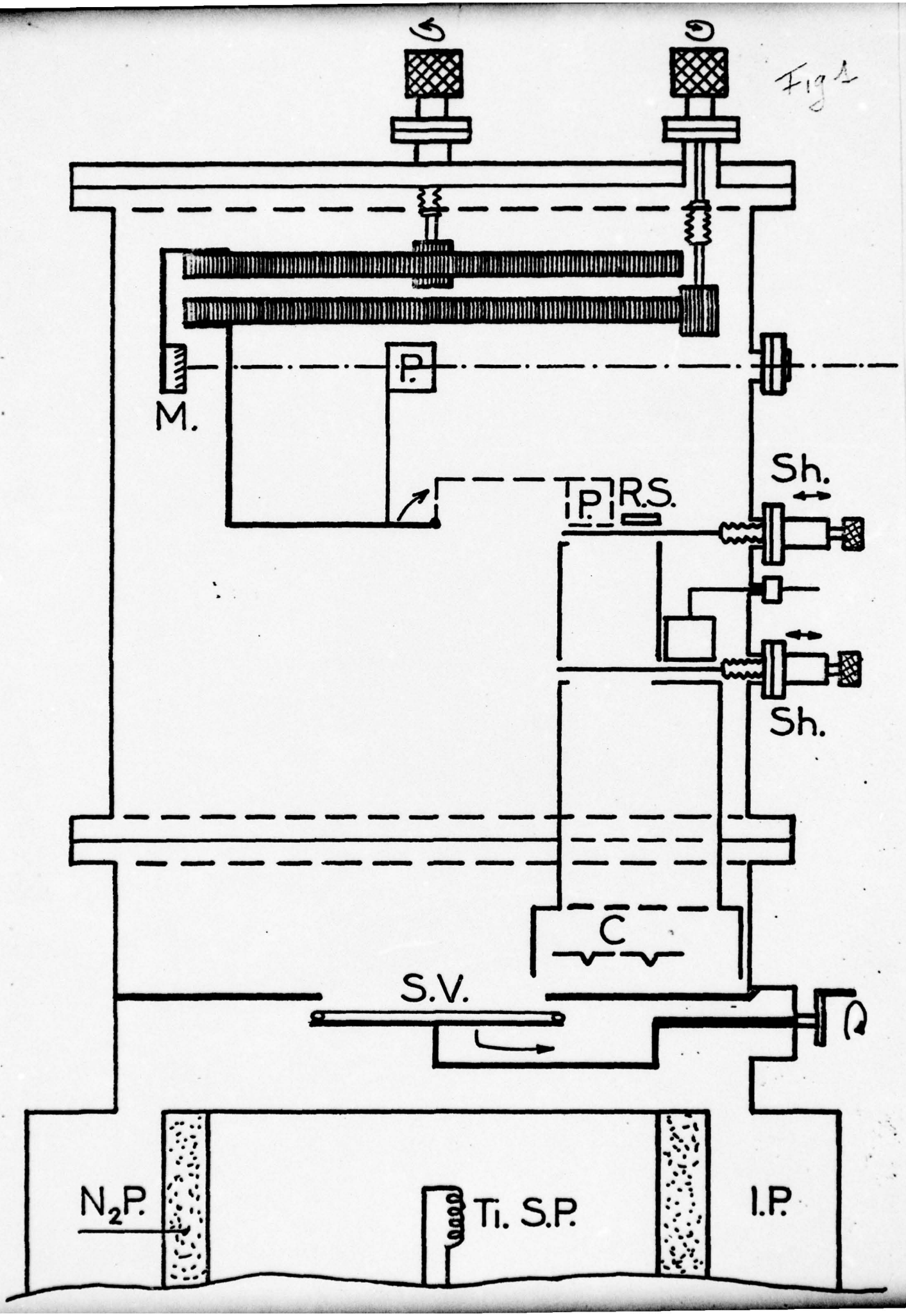

Fig 2

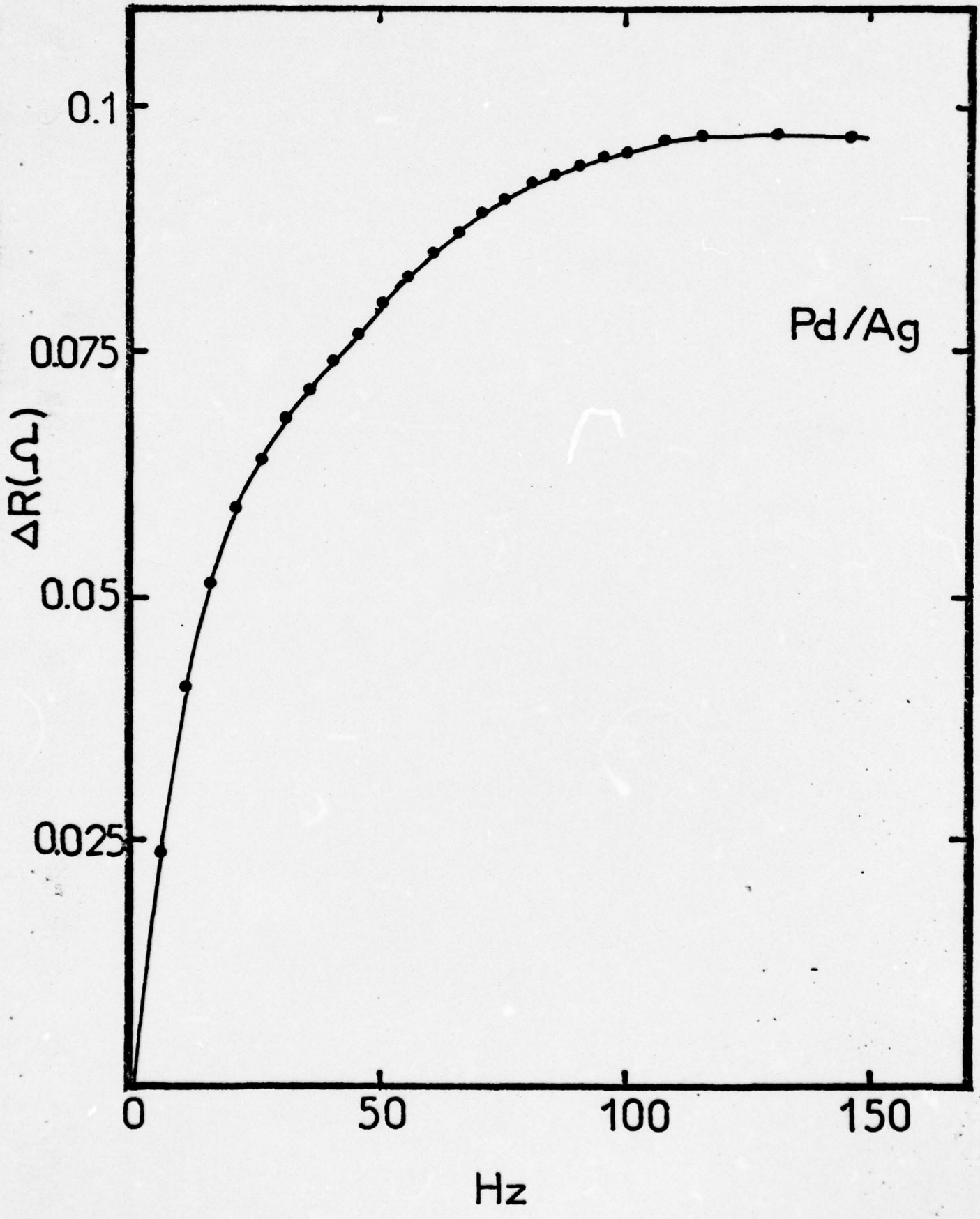

fig 3

M
P
W.P
Ch.
REFERENCE IN
SIGNAL IN (A+B)
REFERENCE IN
3132
C 1
C 1
E 2
D 1
CH 2
CH 1
A/B OUT

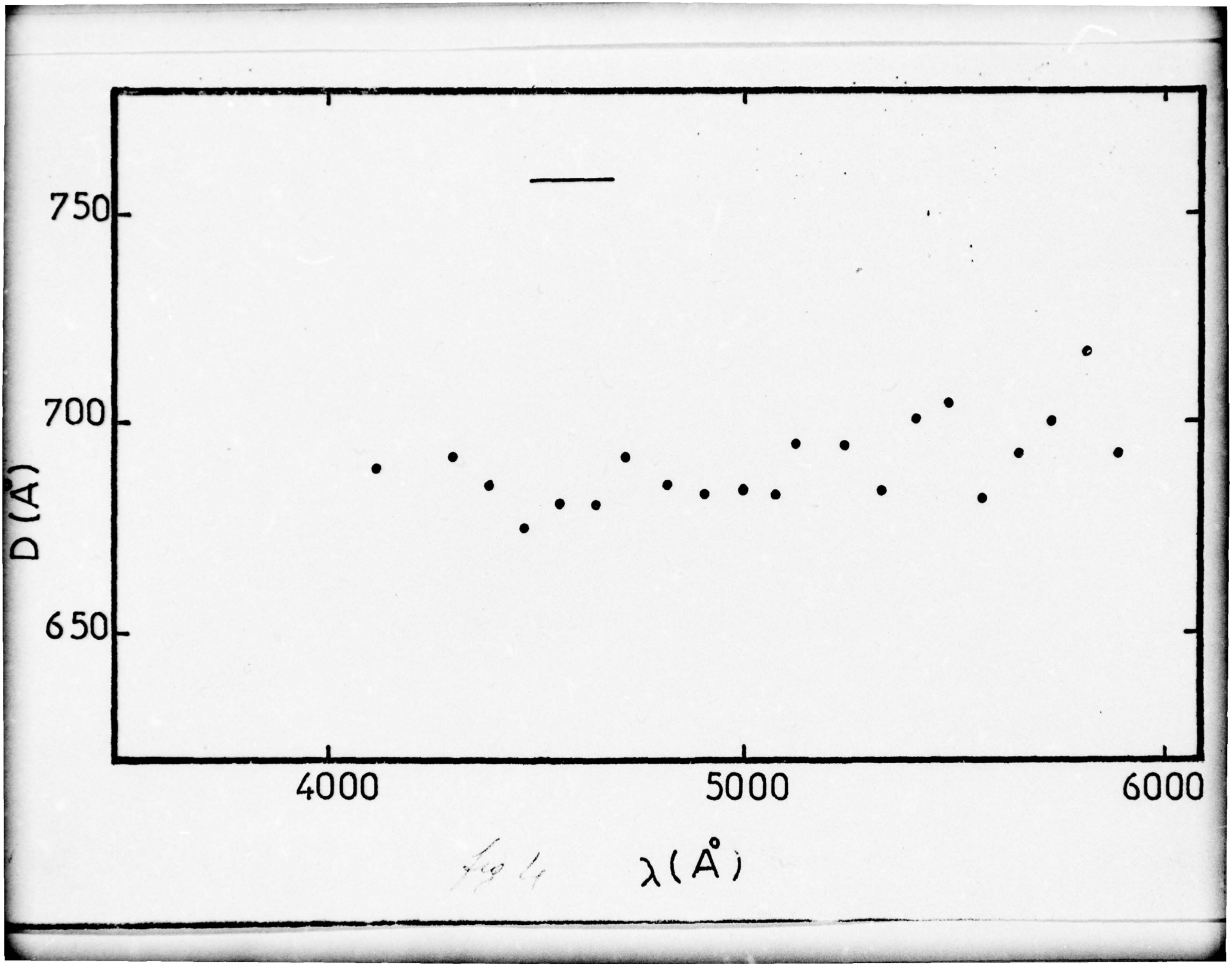

Fig 4

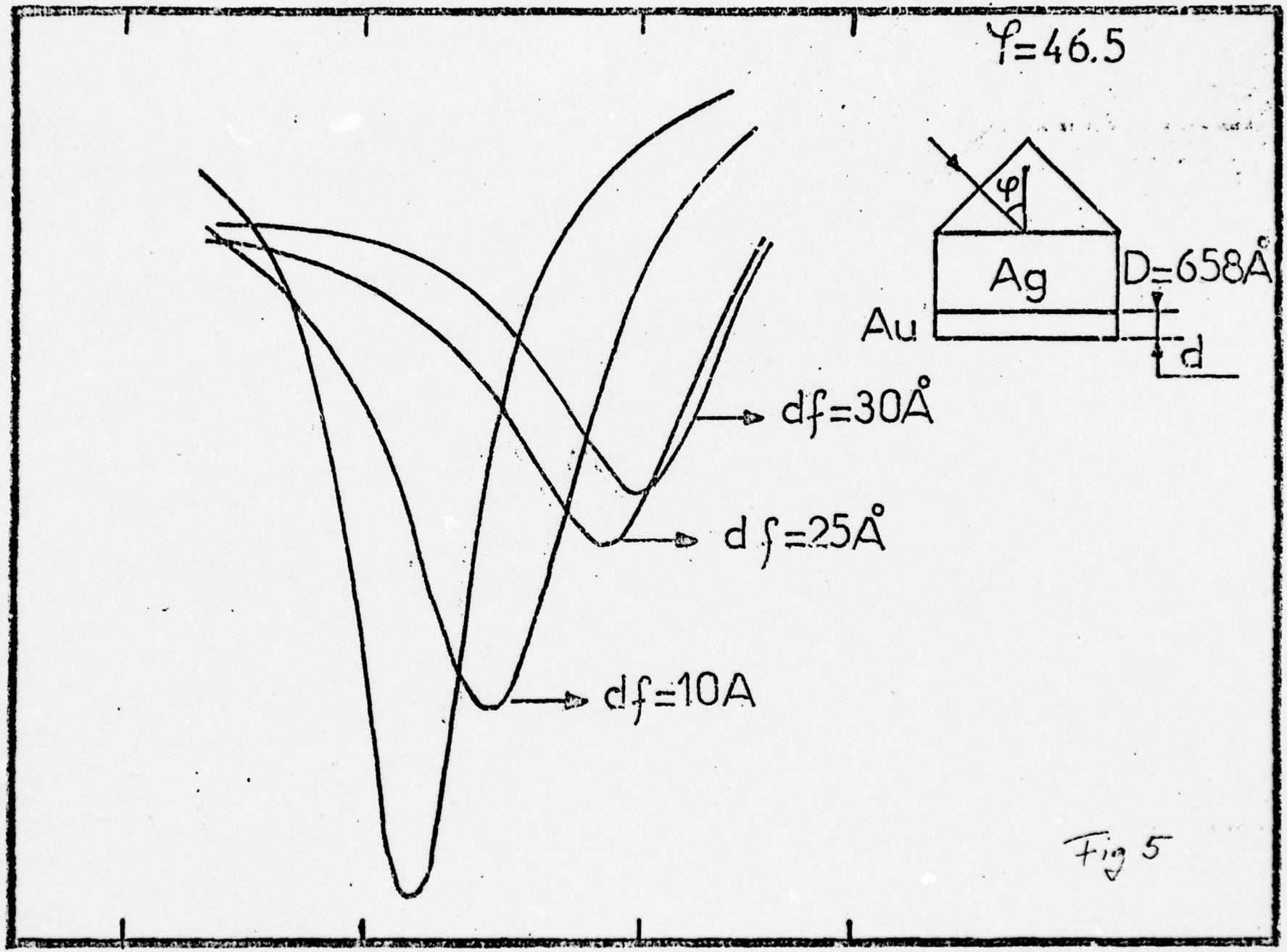
φ=46.5
φ
Ag
Au
D=658Å
d
df=30Å
df=25Å
df=10A
Rp² (arbitrary units)
4200
4600
5000
5400
λ(A)

Fig 5

Fig6

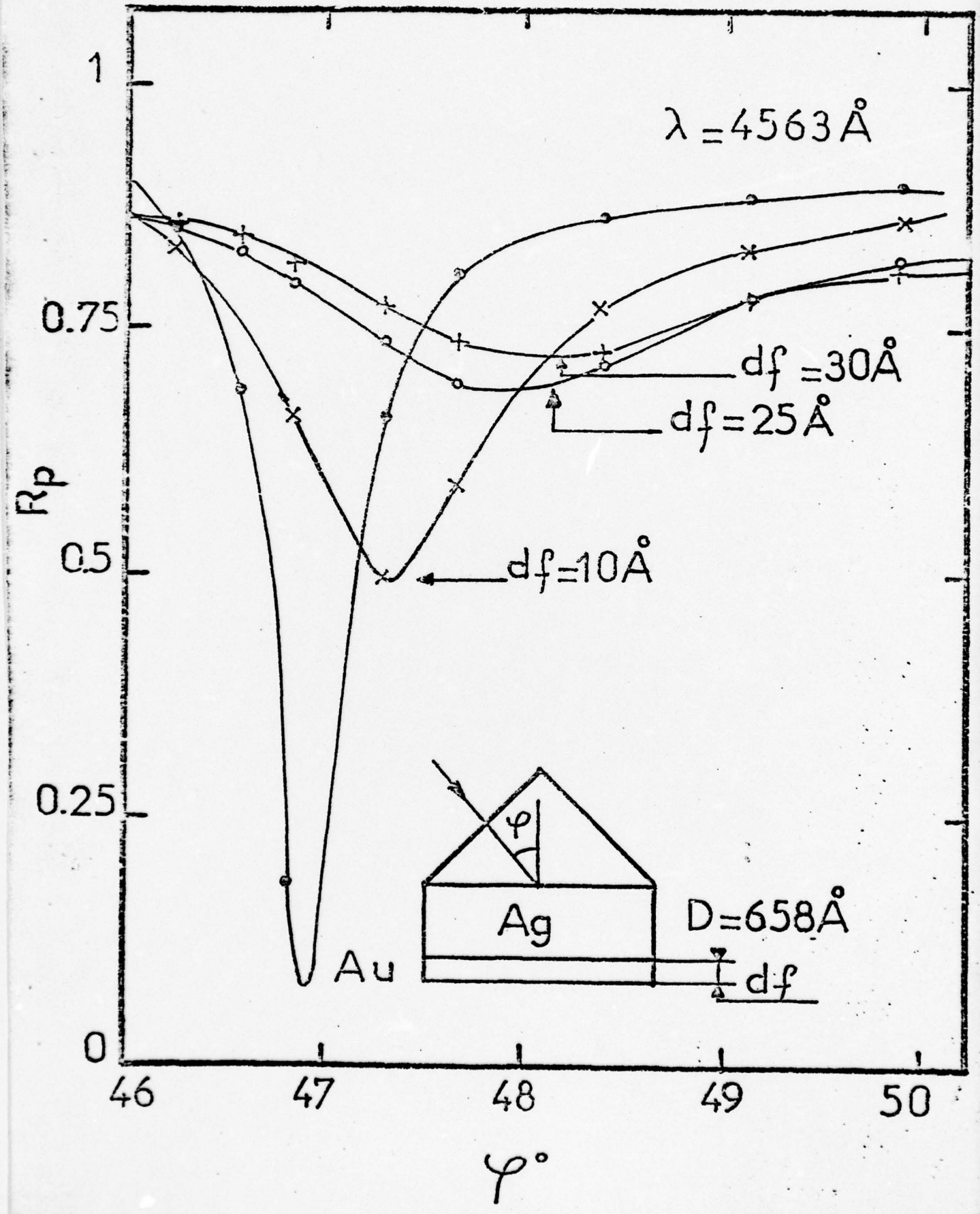
1
0.75
0.5
0.25
0
Rp
λ = 4563 Å
df = 30Å
df = 25Å
df = 10Å
φ
Ag
Au
D = 658Å
df
46
47
48
49
50
φ°

Fig 7

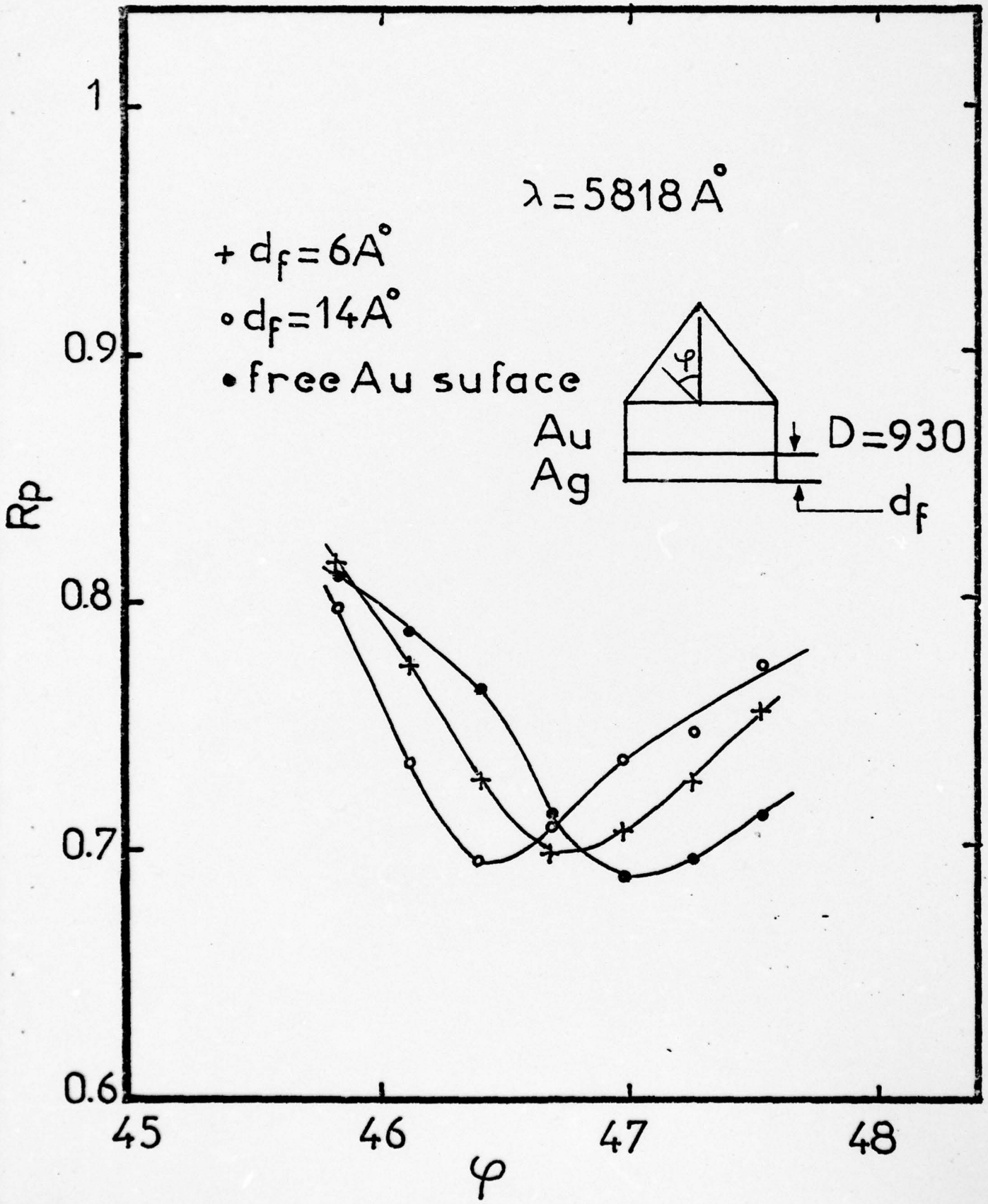
1
0.9
0.8
0.7
0.6
45
46
47
48
R_p
φ
$\lambda = 5818\,\text{Å}$
+ $d_f = 6\text{Å}$
∘ $d_f = 14\text{Å}$
• free Au suface
Au
Ag
D=930
d_f

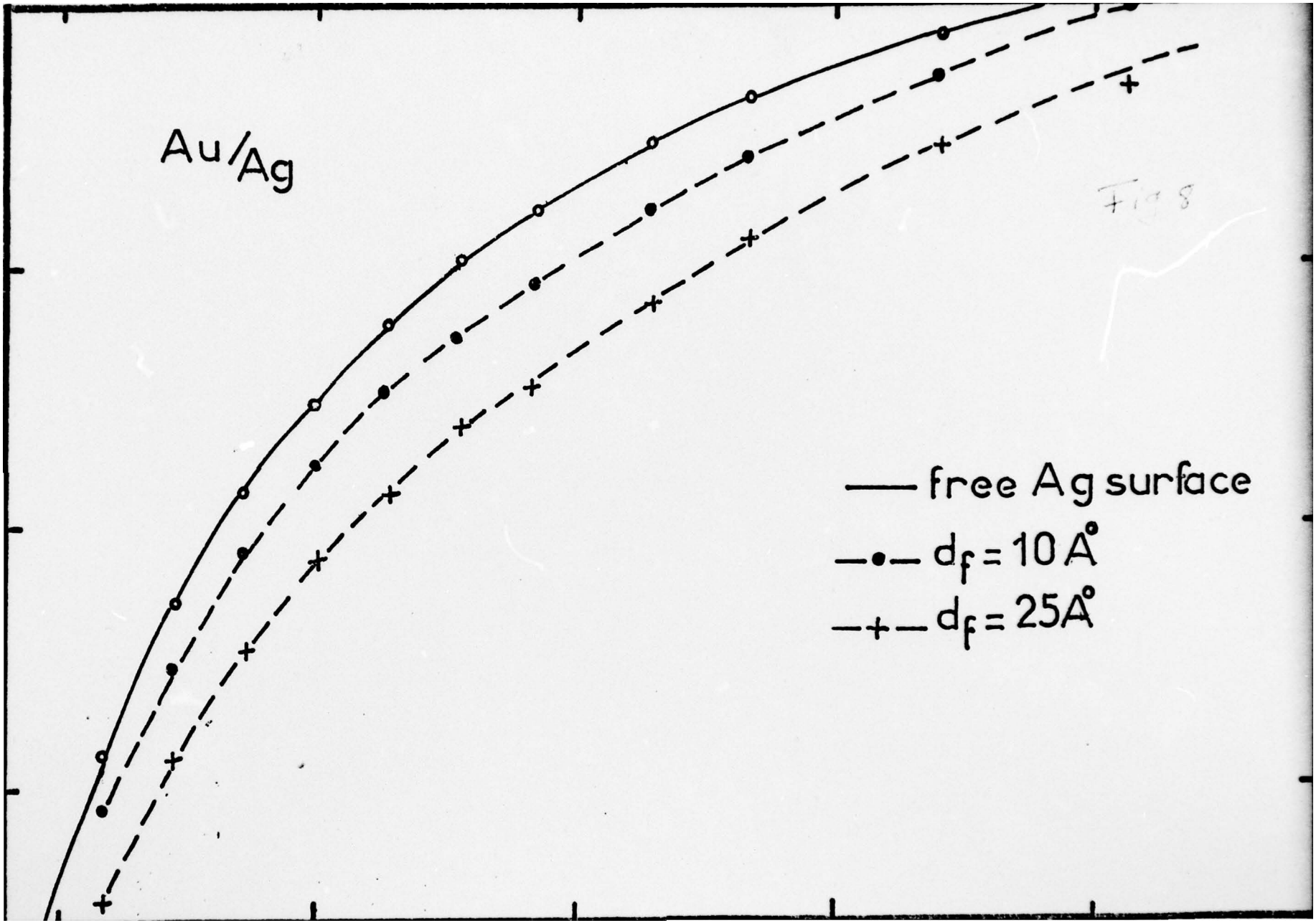
Au/Ag
Fig 8
free Ag surface
$d_f = 10\,\text{Å}$
$d_f = 25\,\text{Å}$

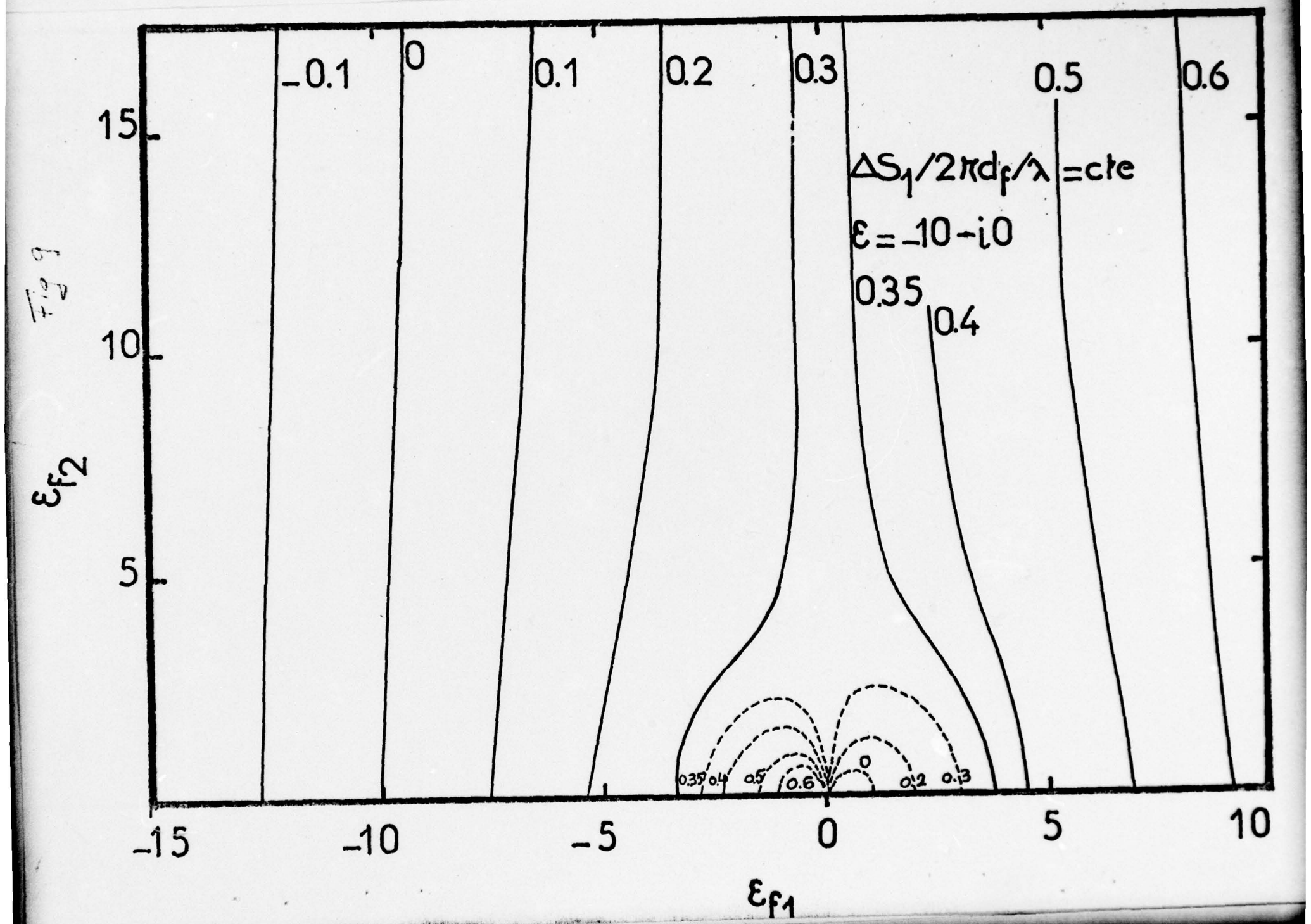
-0.1
0
0.1
0.2
0.3
0.5
0.6
15
10
5
$\Delta S_1/2\pi d_f/\lambda$ = cte
$\varepsilon = -10 - i0$
0.35
0.4
0.35
0.4
0.5
0.6
0
0.2
0.3
ε_{f2}
-15
-10
-5
0
5
10
ε_{f1}

Fig 10

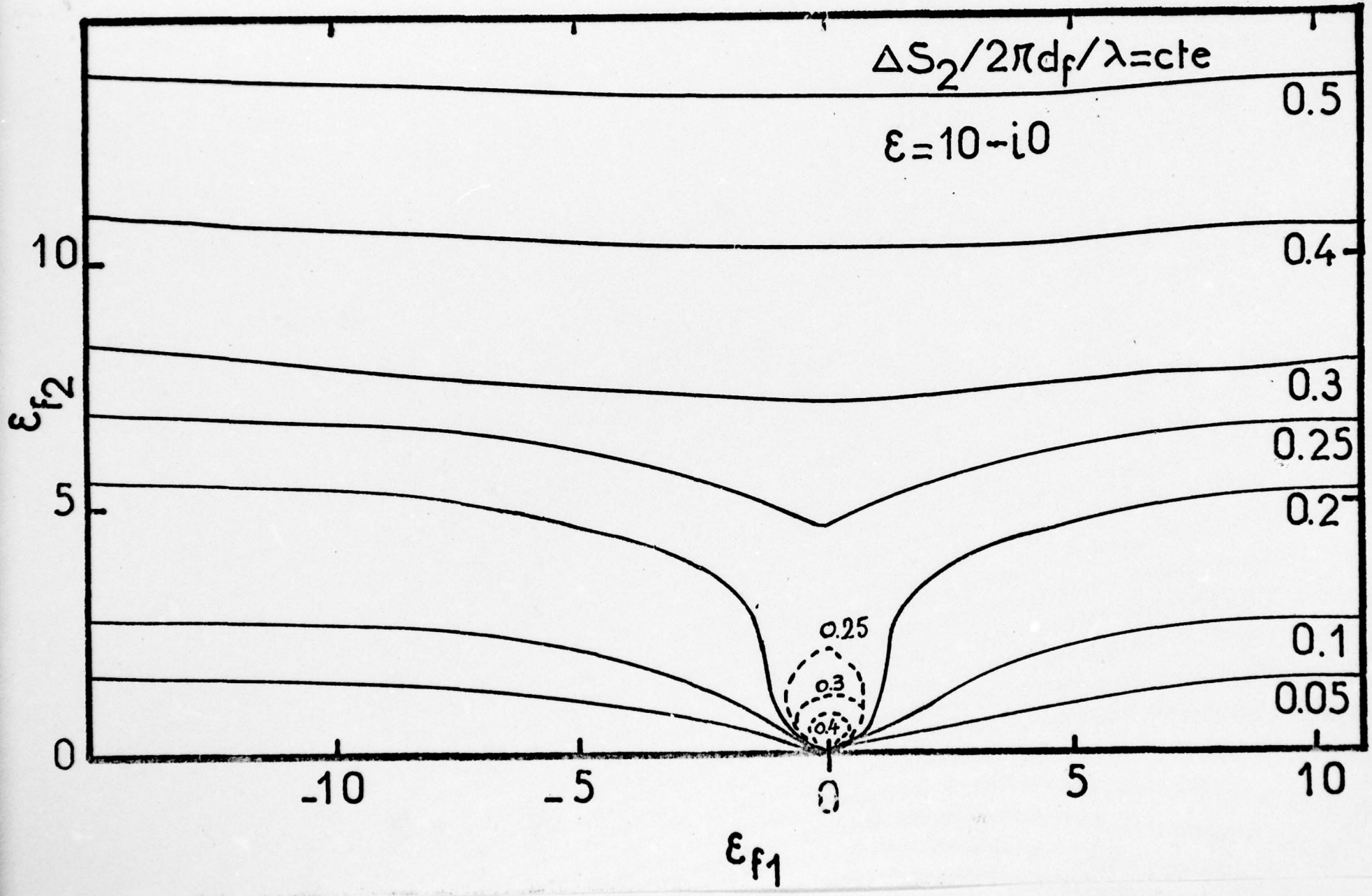
$\Delta S_2/2\pi d_f/\lambda$=cte
ε=10-i0
0.5
0.4
0.3
0.25
0.2
0.1
0.05
0.25
0.3
0.4
10
5
0
ε_{f2}
-10
-5
0
5
10
ε_{f1}

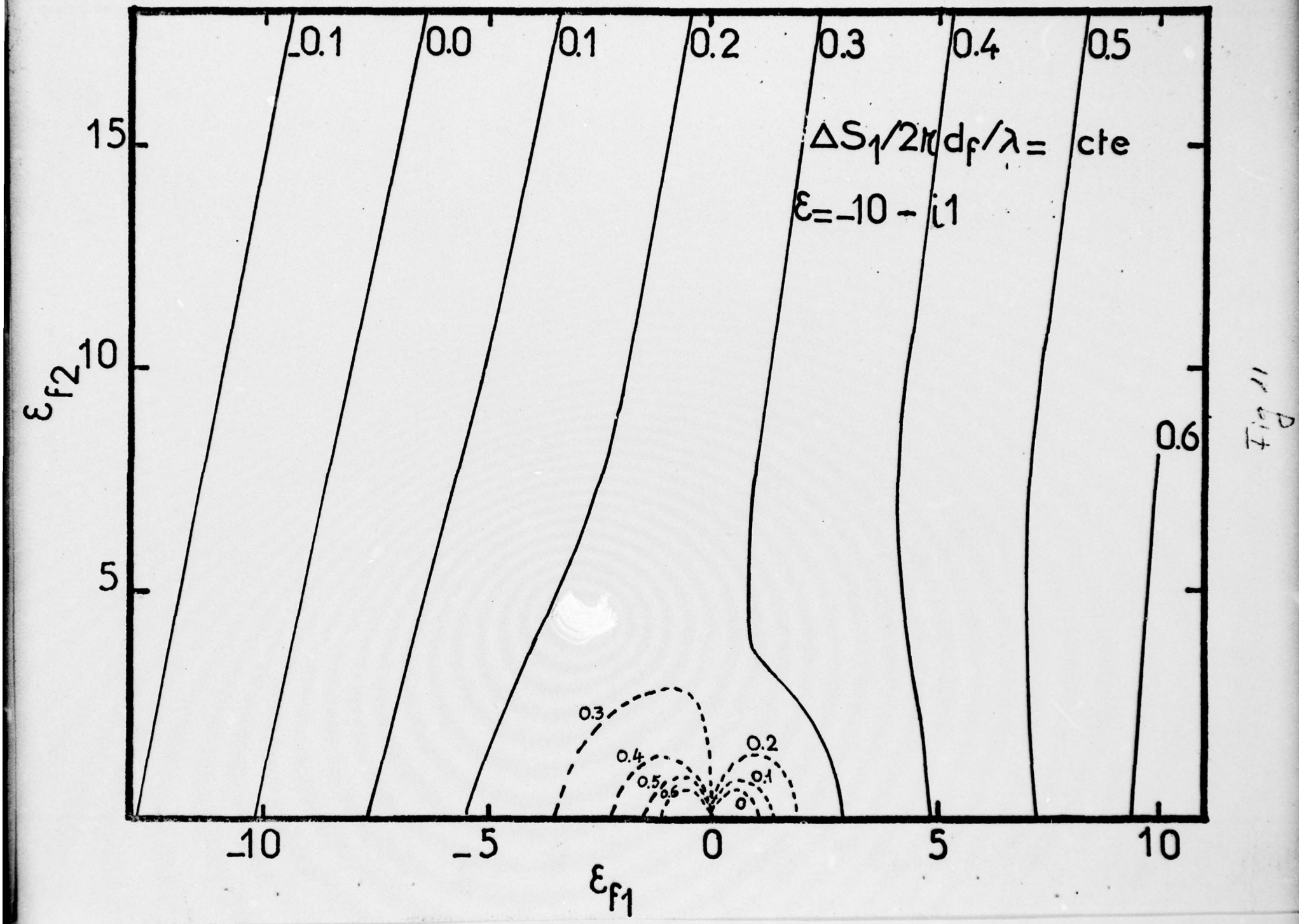
-0.1
0.0
0.1
0.2
0.3
0.4
0.5
0.6
$\Delta S_1/2\pi d_f/\lambda$ = cte
$\varepsilon = -10 - i1$
15
10
5
ε_{f2}
-10
-5
0
5
10
ε_{f1}
0.3
0.4
0.5
0.6
0.2
0.1
0

Fig. 11

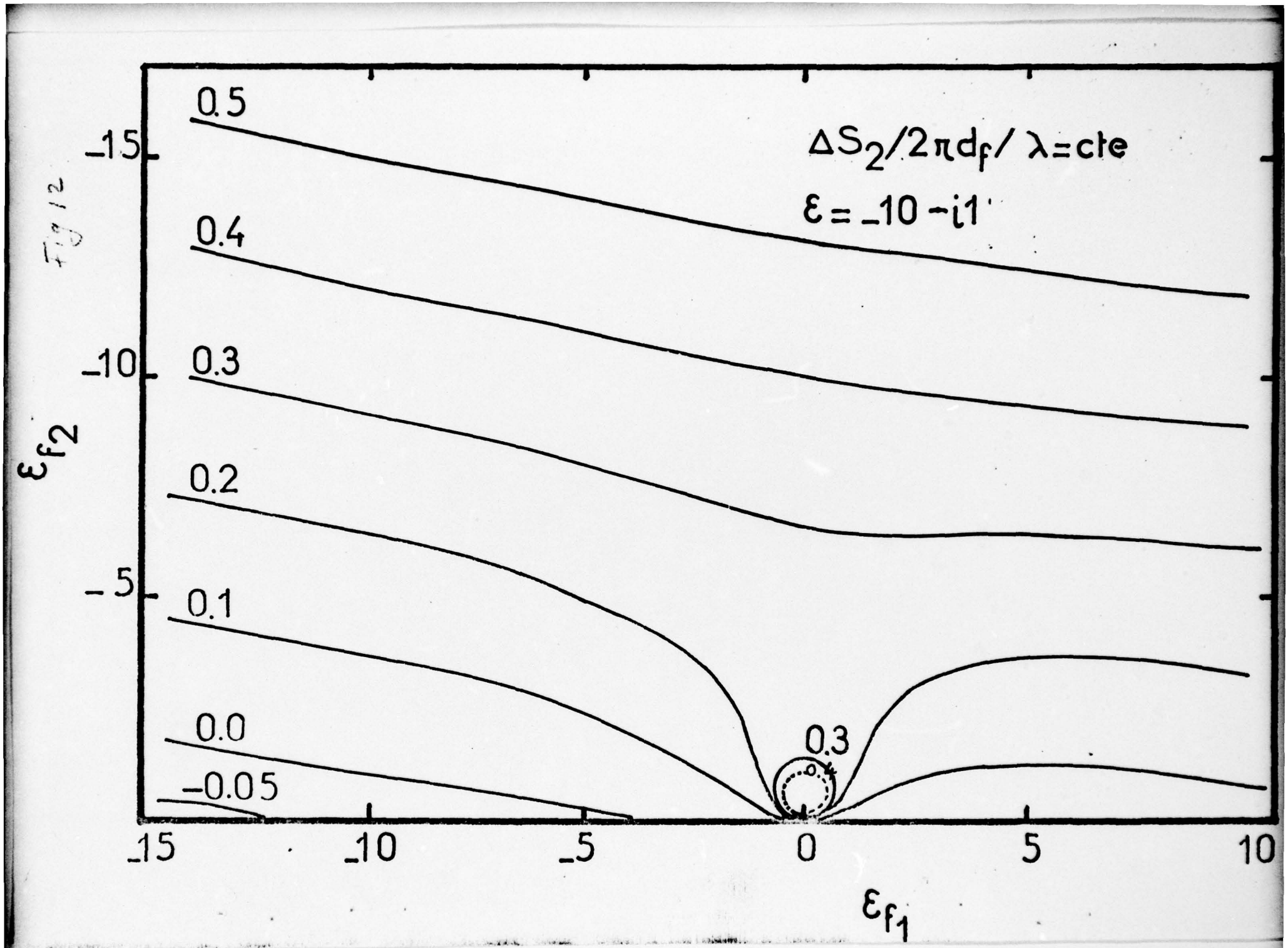
Fig 12
$\Delta S_2/2\pi d_f/\lambda = cte$
$\varepsilon = -10 - i1$
0.5
0.4
0.3
0.2
0.1
0.0
−0.05
0.3
−15
−10
−5
0
5
10
ε_{f_2}
ε_{f_1}

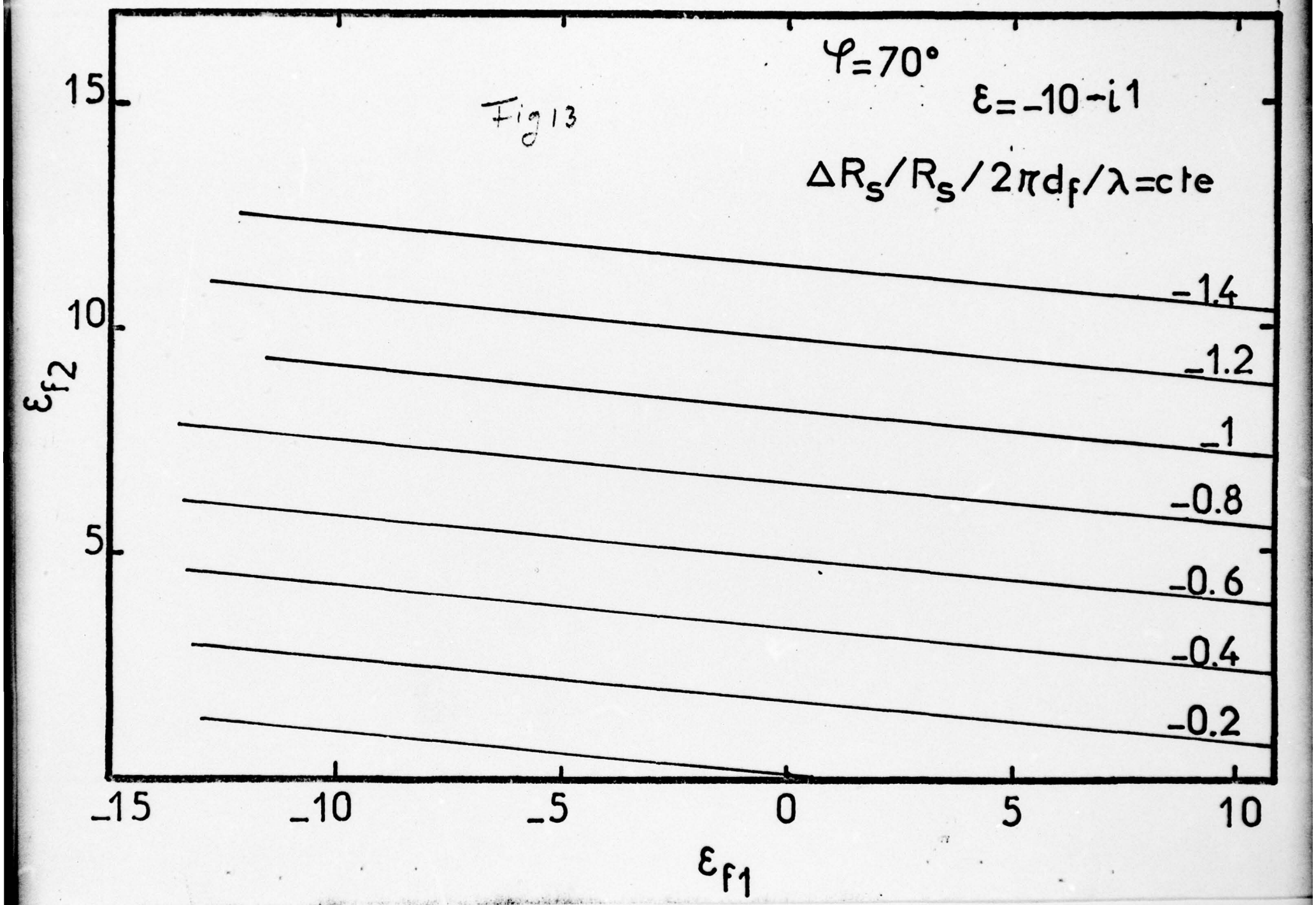
Fig 13
φ=70°
ε=-10-i1
ΔRs/Rs/2πdf/λ=cte
-1.4
-1.2
-1
-0.8
-0.6
-0.4
-0.2
15
10
5
εf2
-15
-10
-5
0
5
10
εf1

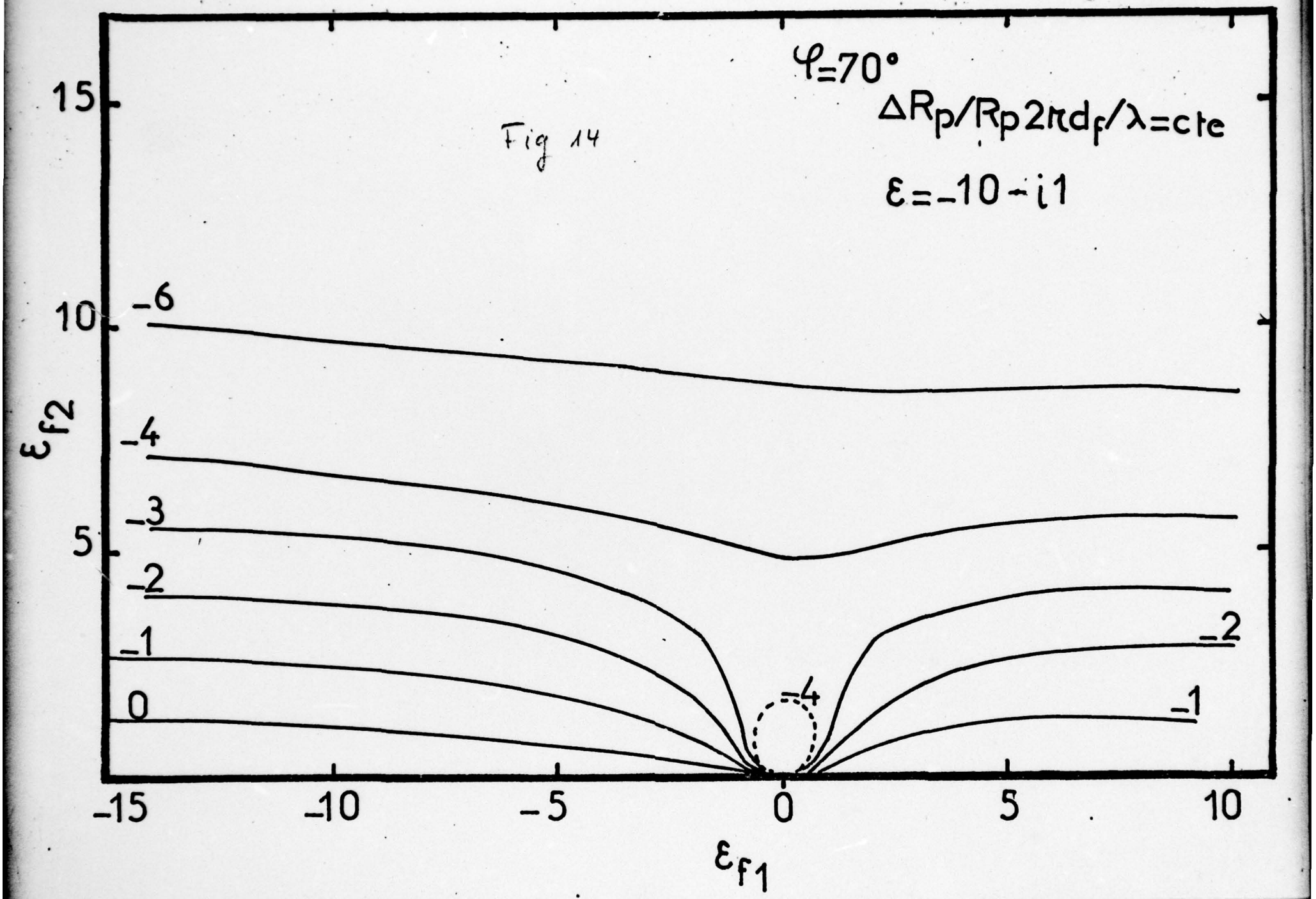
φ=70°
ΔRp/Rp 2πdf/λ=cte
ε=-10-i1
15
10
5
-6
-4
-3
-2
-1
0
-2
-1
-4
εf2
-15
-10
-5
0
5
10
εf1

Fig 14

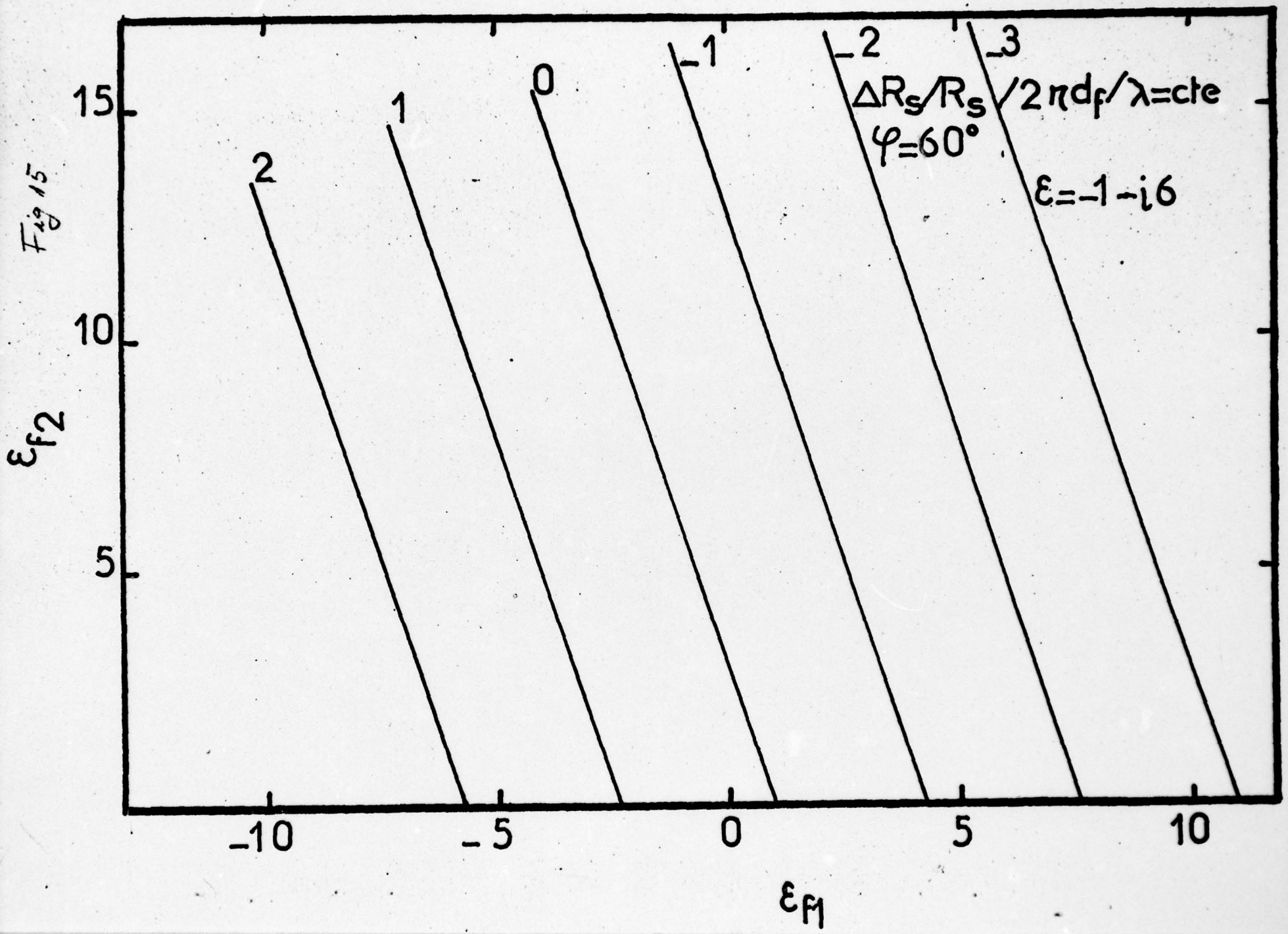
Fig 15
15
10
5
ε_{f2}
2
1
0
-1
-2
-3
$\Delta R_s/R_s$ / $2\pi d_f/\lambda$=cte
φ=60°
ε=-1-i6
-10
-5
0
5
10
ε_{f1}

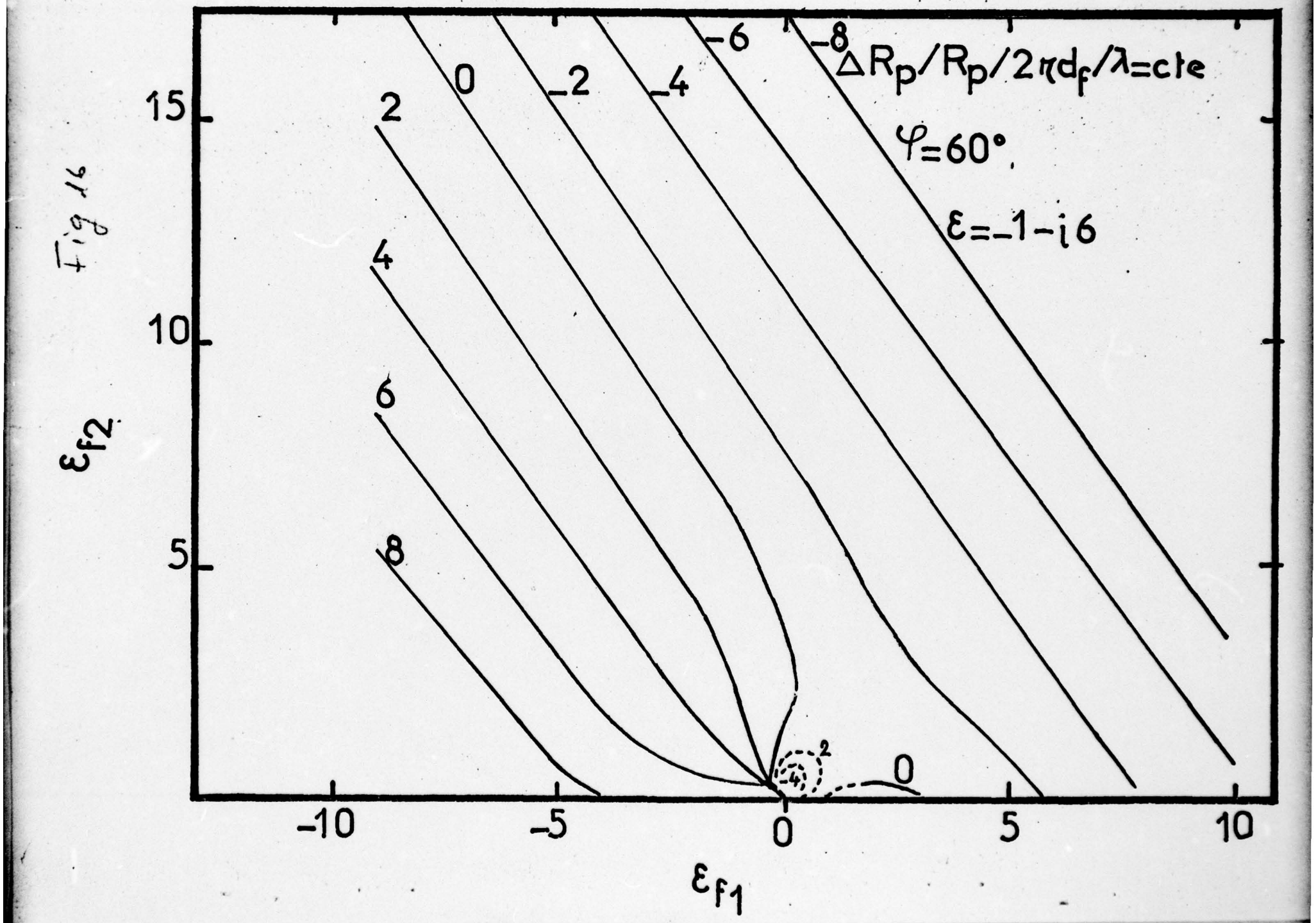
Fig 16
$\Delta R_p/R_p/2\pi d_f/\lambda = cte$
$\varphi = 60°$
$\varepsilon = -1 - i6$
ε_{f2}
ε_{f1}
15
10
5
-10
-5
0
5
10
2
0
-2
-4
-6
-8
4
6
8
2
4
0

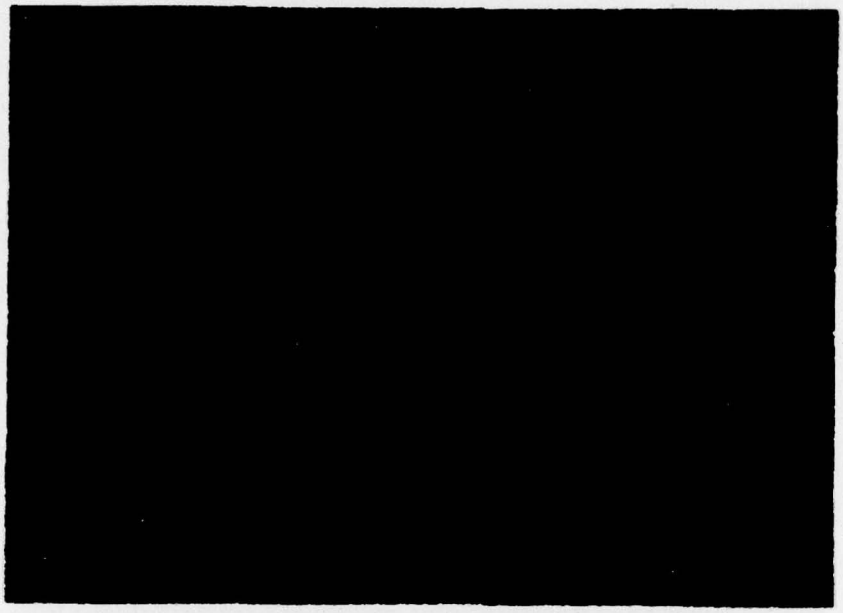

1 μ

Fig 17

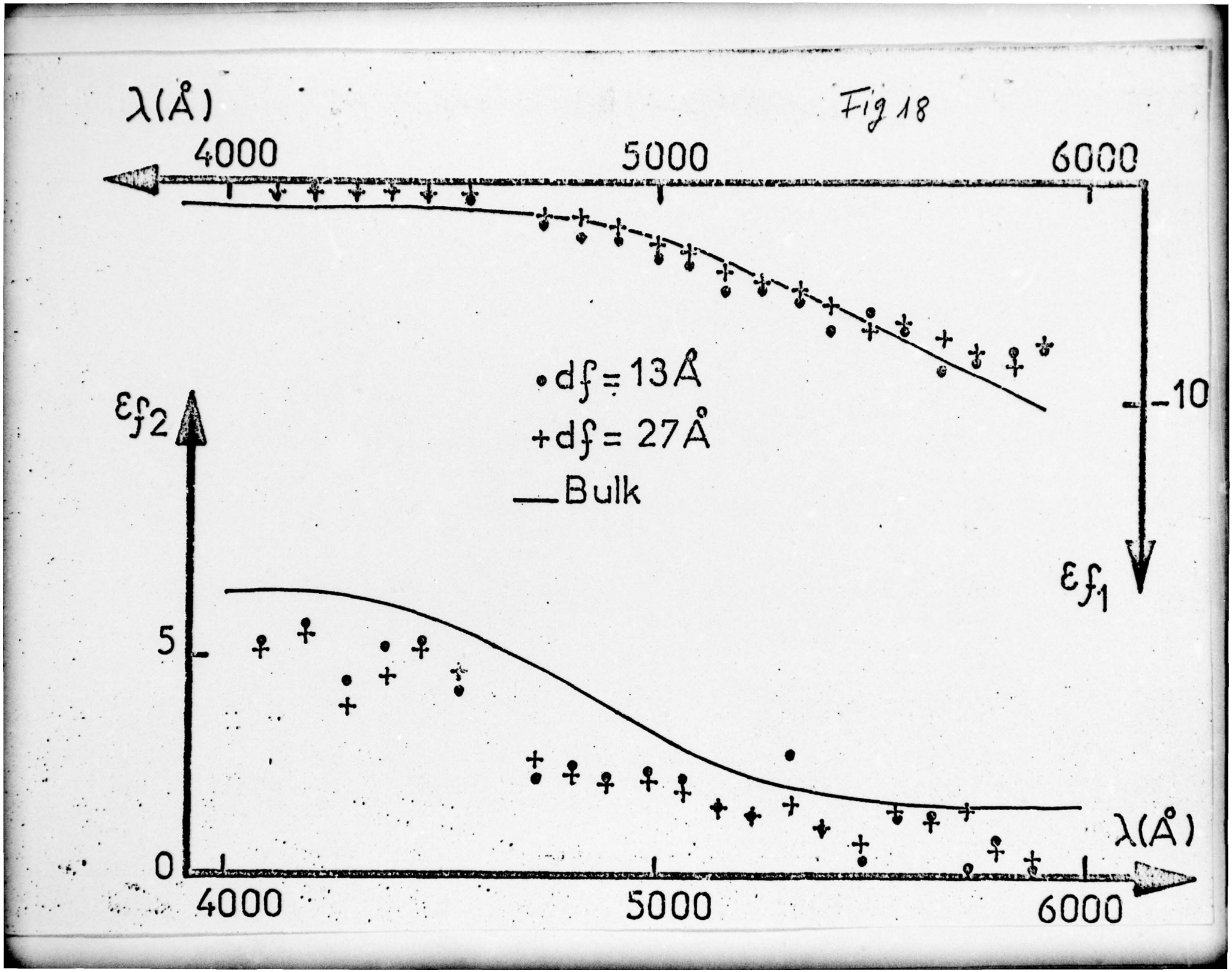
λ(Å)
4000
5000
6000
Fig 18
•df = 13Å
+df = 27Å
—Bulk
−10
ε_{f_1}
ε_{f_2}
5
0
λ(Å)
4000
5000
6000

Fig 19

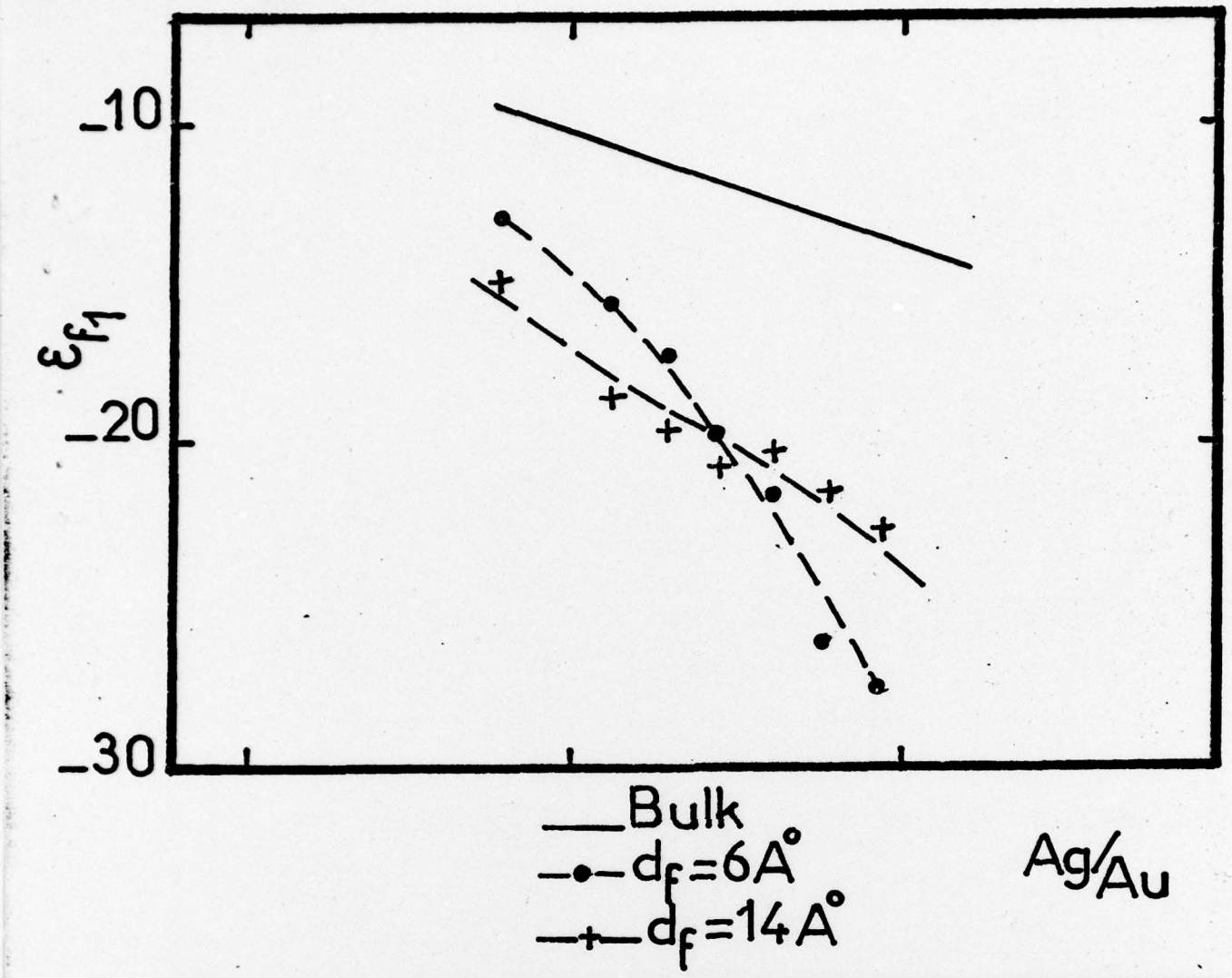
-10
-20
-30
ε_{f1}
Bulk
d_f=6Å
d_f=14Å
Ag/Au

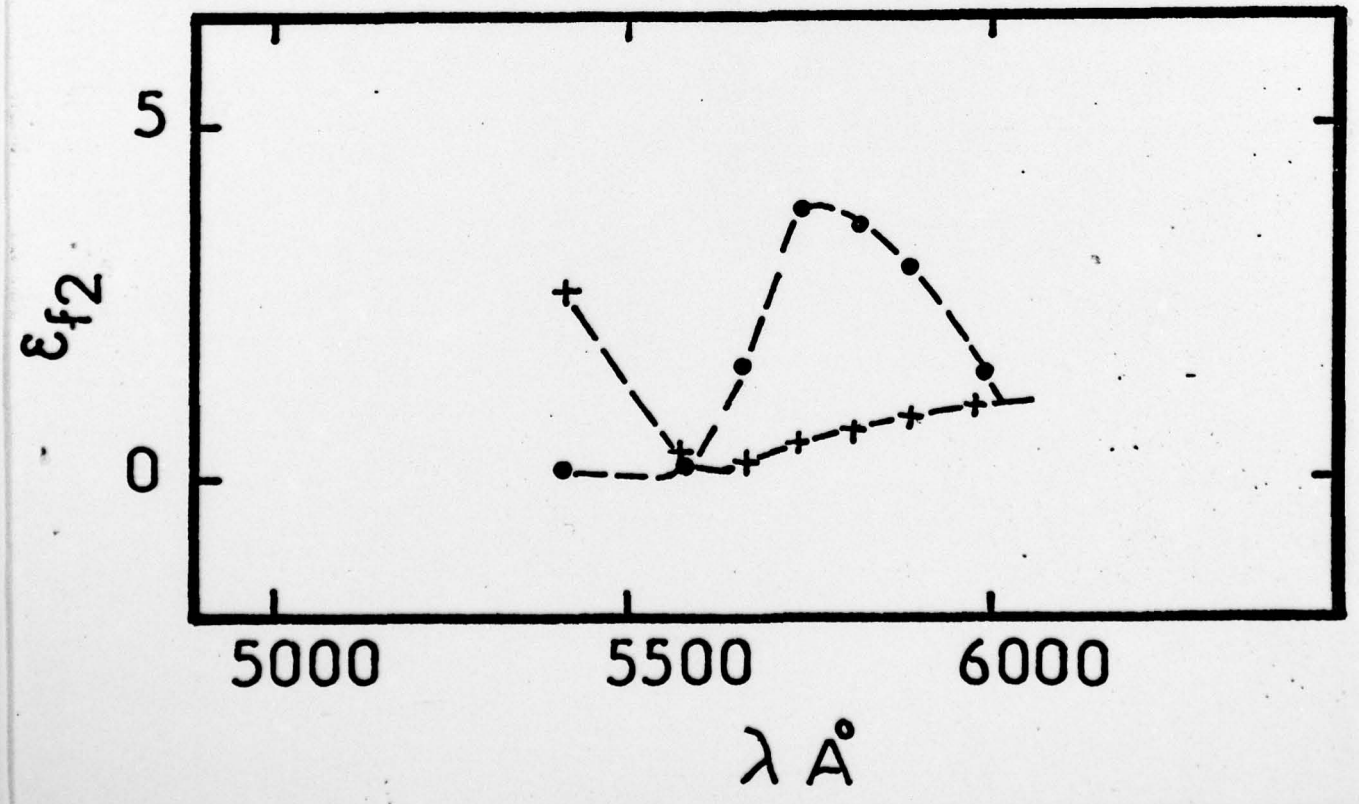
5
0
ε_{f2}
5000
5500
6000
λ Å

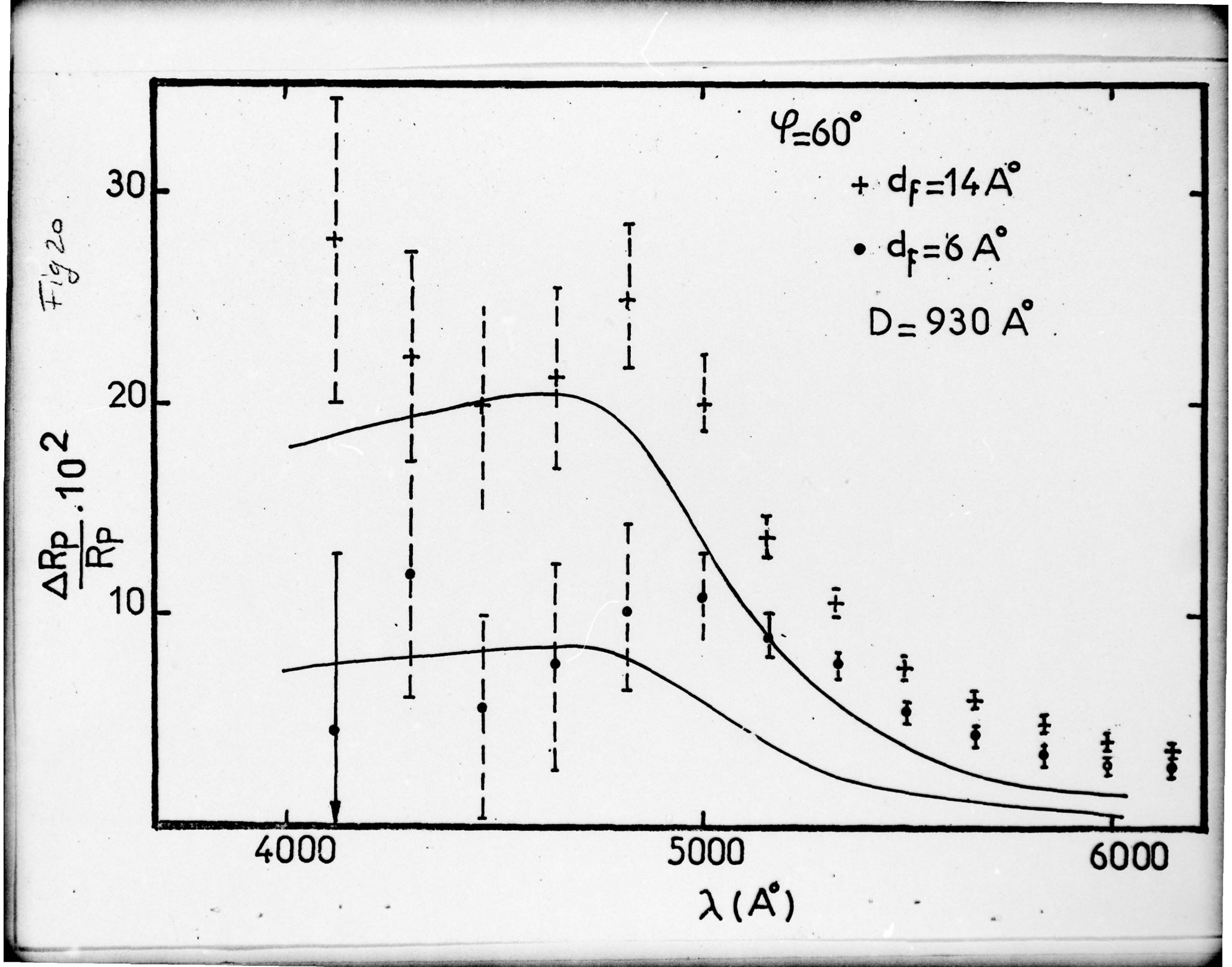
Fig 20
φ=60°
+ d_f=14 A°
• d_f=6 A°
D= 930 A°
$\frac{\Delta R_p}{R_p} \cdot 10^2$
30
20
10
4000
5000
6000
λ (A°)

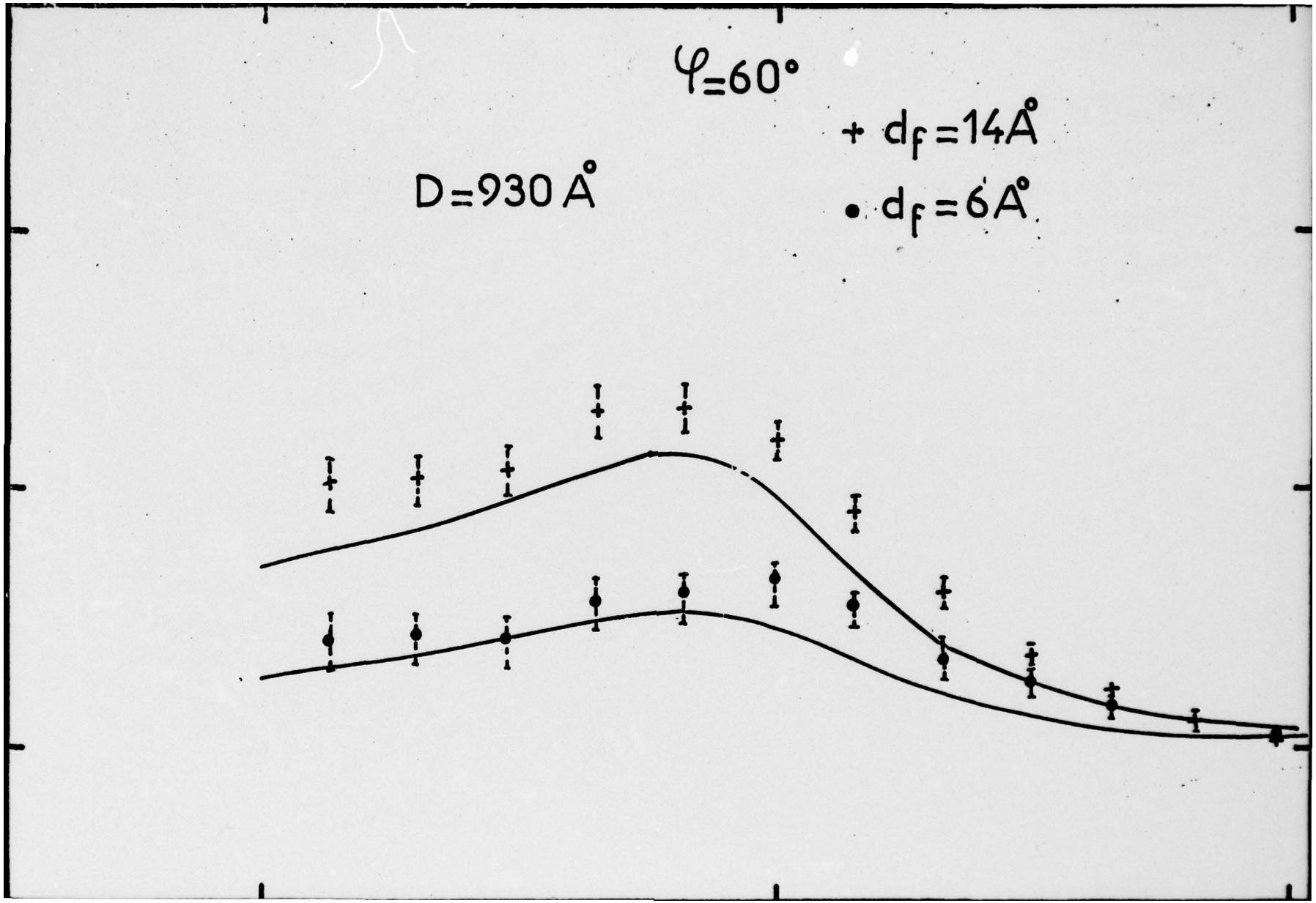
φ=60°
+ d_f=14Å
• d_f=6Å
D=930 Å

UNCLASSIFIED

SECURITY CLASSIFICATION OF THIS PAGE (When Data Entered)

REPORT DOCUMENTATION PAGE

READ INSTRUCTIONS BEFORE COMPLETING FORM

1. REPORT NUMBER

2. GOVT ACCESSION NO.

3. RECIPIENT'S CATALOG NUMBER

4. TITLE (and Subtitle)
INVESTIGATIONS OF SURFACES AND INTERFACES WITH OPTICAL EXCITATION OF SURFACE PLASMONS.

5. TYPE OF REPORT & PERIOD COVERED
ANNUAL TECHNICAL REPORT • MAY 1976 - DECEMBER 1976.

6. PERFORMING ORG. REPORT NUMBER

7. AUTHOR(s)
F. ABELES
T. LOPEZ-RIOS

8. CONTRACT OR GRANT NUMBER(s)
DA-ERO-75-G-027 new

9. PERFORMING ORGANIZATION NAME AND ADDRESS
Laboratoire d'Optique des Solides
Tour 13-12, 4e etage, 4 Place Jussieu,
75230 PARIS CEDEX 05, France

10. PROGRAM ELEMENT, PROJECT, TASK AREA & WORK UNIT NUMBERS
6.11.02A-1T161102B11B-00-491

11. CONTROLLING OFFICE NAME AND ADDRESS
U.S. Army R&S Group (Europe)
Box 65
FPO New York 09510

12. REPORT DATE
DECEMBER 1976

13. NUMBER OF PAGES
49 (12) 36 pp.

14. MONITORING AGENCY NAME & ADDRESS (if different from Controlling Office)

15. SECURITY CLASS. (of this report)
UNCLASSIFIED

15a. DECLASSIFICATION/DOWNGRADING SCHEDULE

16. DISTRIBUTION STATEMENT (of this Report)
APPROVED FOR PUBLIC RELEASE

DISTRIBUTION UNLIMITED

17. DISTRIBUTION STATEMENT (of the abstract entered in Block 20, if different from Report)

18. SUPPLEMENTARY NOTES

19. KEY WORDS (Continue on reverse side if necessary and identify by block number)
PLASMONS; INTERFACES: SURFACES: GOLD AND SILVER FILMS;

OPTICAL PROPERTIES

20. ABSTRACT (Continue on reverse side if necessary and identify by block number)
This report covers the possibility of using the optical excitation of surface plasmons by ATR for the investigation of the metal-electrolyte interface. The method is very sensitive to the modifications of the interface, and it allows studies which are otherwise extremely difficult to perform using classical optical techniques. By the ATR technique, the author investigated the modifications of the complex wave vector of the surface plasmons* and these have a clear physical meaning. This technique was used in performing (Continued...)

6pp next page

DD FORM 1 JAN 73 1473 EDITION OF 1 NOV 65 IS OBSOLETE

* are investigated by the ATR technique

UNCLASSIFIED

SECURITY CLASSIFICATION OF THIS PAGE (When Data Entered)

406 163

20. Abstract (Continued...)

potentiometric and optical studies of Au-electrolyte interfaces; both polarization at the interface between gold and $H_2SO_4^-$ and $HClO_4^-$ solutions, and also the anodic oxidation of gold in $H_2SO_4^-$ were investigated.